Trinity College Dublin
Coláiste na Tríonóide, Baile Átha Cliath
The University of Dublin

# The role of canonical and non-canonical inflammasomes in a model of oxidative stress-induced retinal degeneration

*March 2024*

Eoin Silke, BA (Mod. Hons) MB BAO BCh (Dubl.)

Student number: 07551436

This thesis is submitted to Trinity College Dublin, the University of Dublin, in fulfilment of the degree of MSc in Clinical Medicine

Department of Clinical Medicine, School of Medicine, Trinity College Dublin

Thesis supervisor: Dr Sarah Doyle

**Declaration**

*I declare that this thesis has not been submitted as an exercise for a degree at this or any other university and it is entirely my own work.*

*I agree to deposit this thesis in the University's open access institutional repository or allow the Library to do so on my behalf, subject to Irish Copyright Legislation and Trinity College Library conditions of use and acknowledgement.*

*I consent to the examiner retaining a copy of the thesis beyond the examining period, should they so wish (EU GDPR May 2018).*

_____

## Acknowledgements

I would like to acknowledge the enormous support and persistence of Dr Sarah Doyle throughout her supervision of this work. I would also like to acknowledge the support of Mr Mark Cahill, consultant vitreoretinal surgeon in the Royal Victoria Eye and Ear Hospital, Dublin, who facilitated this opportunity in collaboration with Dr Doyle. They have both provided me with immeasurable guidance and training in both my academic and clinical career. I would like to thank the Research Foundation of the Royal Victoria Eye and Ear Hospital for providing financial support for this endeavour. In addition I am very grateful for the assistance of other researchers working in Trinity, including Dr Matthew Campbell, Dr Kiva Brennan, Dr Erin Fahey, and Dr Rebecca Mahony, and above all Dr Ema Ozaki and Dr Kelly Mulfaul.

## Summary

Retinal degenerative diseases like age-related macular degeneration (AMD) are a leading cause of visual impairment. Oxidative stress is known to be important in the pathogenesis of AMD, and oxidative-stress induced retinal degeneration can be studied using various models. The sodium iodate mouse is a widely used animal model of retinal degeneration, but its pathobiology is not well understood. Activation of innate immune pathways is suspected to play an important role in retinal degeneration secondary to oxidative stress. We investigated both canonical and non-canonical inflammasomes in sodium iodate-induced retinal degeneration in two types of genetic knockout mice (*Pycard*$^{-/-}$ and *Casp11*$^{-/-}$). *Pycard*$^{-/-}$ mice are deficient in ASC protein which prevents the majority of canonical inflammasomes from forming, whereas deficiency in caspase-11 prevents non-canonical inflammasome activation. Using *in vivo* optical coherence tomography measurements, histological analysis, and TUNEL staining we observed that in *Pycard*$^{-/-}$ mice, loss of canonical inflammasome formation did not appear to affect oxidative stress-induced retinal damage. However, knocking out caspase-11 and thus inhibiting non-canonical inflammasome pathways may limit oxidative stress-induced retinal degeneration.

# Abbreviations

| | |
|---|---|
| AAV | Adeno-associated virus |
| AIM | Absent-in-melanoma |
| ALR | AIM-2-like receptor |
| AMD | Age-related macular degeneration |
| ARPE-19 | Human retinal pigment epithelial cell line |
| ARVO | The Association for Research in Vision and Ophthalmology |
| ASC | Apoptosis-associated speck-like protein containing a CARD |
| BRB | Blood-retinal barrier |
| C1q | Complement component 1q |
| C3 | Complement component 3 |
| C57BL/6J | A mouse strain |
| CARD | Caspase activation and recruitment domain |
| Ccl2 | Chemokine (C-C motif) ligand 2 |
| CEP | Carboxyethyl pyrrole |
| CFH | Complement factor H |
| CNV | Choroidal neovascularisation |
| CX3CR1 | CX3C motif chemokine receptor 1 |
| DNA | Deoxyribonucleic acid |
| ERG | Electroretinogram |
| FIIND | Function to find domain |
| GCL | Ganglion cell layer |
| GFP | Green fluorescent protein |
| GSDMD | Gasdermin D |
| H&E | Haematoxylin and eosin |
| HIN | Haematopoietic interferon-inducible nuclear protein domain |
| HNE | 4-Hydroxynonenal |
| IL-1β | Interleukin 1β |
| INL | Inner nuclear layer |
| IPL | Inner plexiform layer |
| LPS | Lipopolysaccharide |
| LRR | Leucine-rich repeat domain |
| MnSOD | Manganese superoxide dismutase |
| mRNA | Messenger RNA |
| NACHT | NTPase domain present in NAIP, CIITA, HET-E, and TP-1 |
| $NaIO_3$ | Sodium iodate |
| NAIP | NLR family apoptosis inhibitory protein |
| NLR | NOD-like receptor |
| NLRC4,5 | NLR family CARD domain-containing protein 4 |
| NLRP1,2,3,5,6,7,12 | NLR family pyrin-domain containing |
| NOD | Nucleotide oligomerisation domain |
| OCT | Optical coherence tomography<br>*or* Optimal cutting temperature |
| ONL | Outer nuclear layer |

| | |
|---|---|
| OPL | Outer plexiform layer |
| PBS | Phosphate buffered saline |
| POS | Photoreceptor outer segment |
| PYD | Pyrin domain |
| RIPK3 | Receptor-interacting serine/threonine-protein kinase 3 |
| ROS | Reactive oxygen species |
| RNA | Ribonucleic acid |
| RNFL | Retinal nerve fibre layer |
| RPE | Retinal pigment epithelium |
| Sarm | Sterile alpha and armadillo motif-containing protein |
| Sod1,2 | Superoxide dismutase |
| TCD | Trinity College Dublin |
| TIR | Toll/IL-1 receptor |
| TUNEL | Terminal deoxynucleotidyl transferase dUTP nick end labeling |
| VEGF | Vascular endothelial growth factor |
| Z-VAD-FMK | Carbobenzoxy-valyl-alanyl-aspartyl-[O-methyl]- fluoromethylketone |
| 661W | Mouse photoreceptor cell line |

# Table of contents

# 1. Introduction

Degenerative diseases of the retina, including age-related macular degeneration (AMD), represent a significant cause of visual morbidity world-wide (Pascolini & Mariotti, 2012). In the Republic of Ireland, the prevalence of AMD has been estimated at 7.2% in those over 50, and it is the predominant cause of sight loss in those over 50 in developed countries (Akuffo *et al.*, 2015). Animal models are important to the study of these diseases, and one such model, the sodium iodate mouse, has been widely used in recent years.

## 1.1 The retina (Figure 1.1)

The retina is the layer of light-sensitive tissue at the posterior aspect of the eye present in most vertebrates. It is highly organised and requires tight regulation of its microenvironment in order to carry out its function (Hoon *et al.*, 2014). In brief, its composition from its outer aspect (ie closer to the scleral wall of the eye) to its inner aspect (ie closer to the vitreous cavity) consists of a layer of light-sensitive photoreceptor cells, which synapse with layers of bipolar cells and other interneurons, which themselves synapse with ganglion cells in the inner retina. The visual information encoded by ganglion cells is transmitted via the optic nerve to the brain.

The photoreceptors are divided into two main groups: rods and cones. Rod cells are more numerous at the peripheral retina and mainly convey night and peripheral vision, as they function better in lower light levels. A central area of the retina called the macula is

particularly dense in cone cells, which detect fine detail and colour. At the very centre of the macula, an area called the fovea has a very high density of cone cells.

The retinal pigment epithelium (RPE), which is present at the outer aspect of the photoreceptors, consists of cuboidal epithelial cells arranged in a monolayer. These RPE cells are particularly rich in melanin pigments. They form a functional unit with the retina (also called the neurosensory retina), and in particular with the photoreceptors.

The RPE has many functions in maintaining the health of the retina, many of them related to homeostasis of the retinal microenvironment. Photoreceptors shed their outer segments (photoreceptor outer segments, or POS) throughout the day as they accumulate toxic byproducts as a result of their light-sensing function (Kocaoglu *et al.*, 2016). These are continually phagocytosed by the RPE so as not to amass in the subretinal space. The outer blood-retinal barrier (oBRB) is also maintained by the RPE: nutrients are transported inwards towards the retina by the RPE, while metabolic end products, ions, and water are delivered outwards (Strauss, 2005). Another important role performed by the RPE is participating in the visual cycle, in which the chromophores which are used up in visual phototransduction are subsequently recycled and returned for use again.

Metabolic support for the retina comes from a dual blood supply, via the central retinal artery and its branches to the inner retina, and the capillary network in the choroid to the outer retina. The choroid is an area of connective tissue which is found between the RPE and the scleral wall of the eye. It possesses highly fenestrated vessels at the level of the choriocapillaris, which is its capillary layer. This permits free exchange of nutrients and

oxygen. Cellular migration however is limited by Bruch's membrane, a thin layer of connective tissue interposed between the choriocapillaris and the RPE (Fields *et al.*, 2020).

Human retinal anatomy as described in the preceding paragraphs differs from the retinal anatomy of other animals, which is relevant as much retinal research has been performed in mice. The overall density of photoreceptors is much greater throughout the human retina when compared with the mouse (Volland *et al.*, 2015). The most important structural difference is the absence in the mouse of the specialised central region of the retina known as the macula. The mouse retina, while it does have an increased concentration of cone cells towards its central region, does not have the sharp peak of cone photoreceptors corresponding to the human central fovea (foveola). Nevertheless, outside the very central 10 degrees of the human macula, the rod-cone ratios are similar between the human macula and the mouse central retina, a finding which lends support to the use of mouse models in preclinical macular research (Volland *et al.*, 2015).

In many diseases of the retina, as in experimentally induced retinal damage like sodium iodate, the death of photoreceptors is the main cause of irreversible visual loss. However, because of the close association of photoreceptor and RPE, disturbances to the RPE as the primary inciting event can also result in secondary damage to the neurosensory retina. We will discuss this further, both in the context of AMD and in the sodium iodate mouse model.

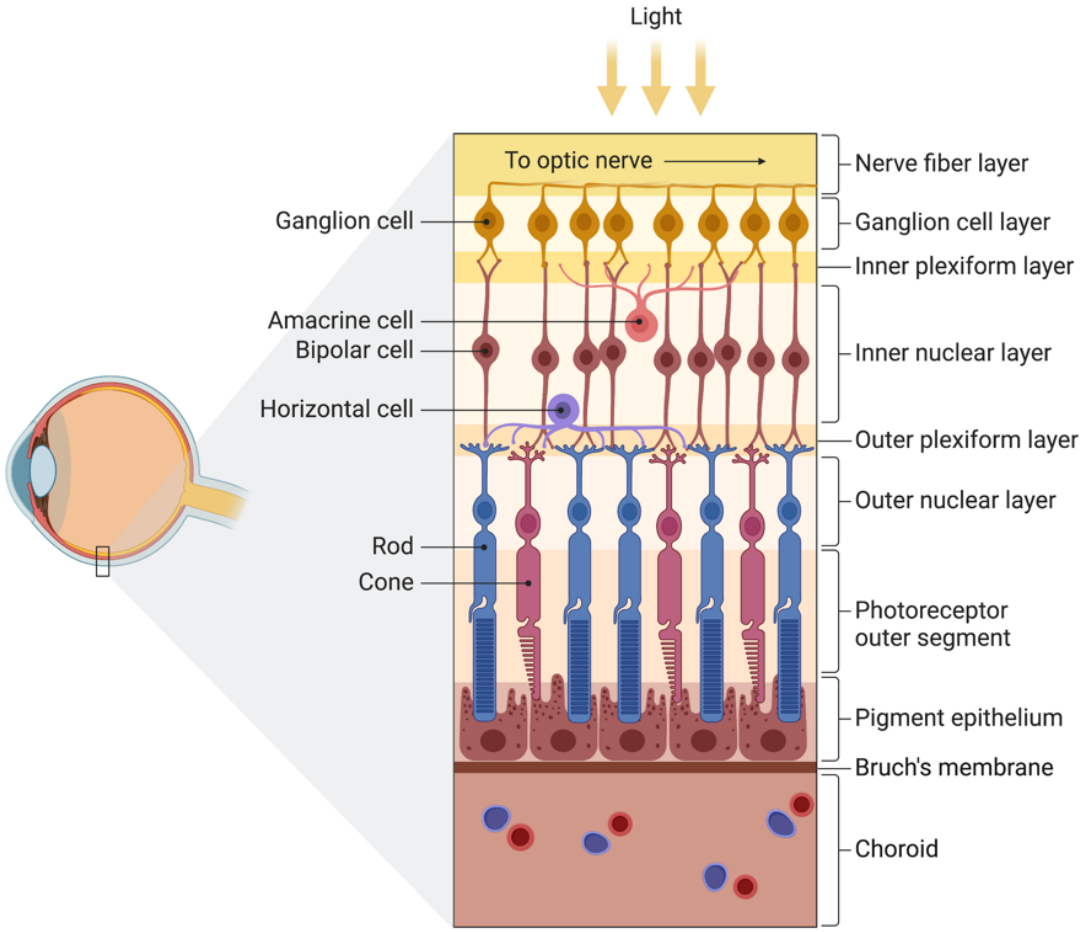


**Figure 1.1 The structure of the retina.**

Incident light passes through the inner structures of the retina to reach the photoreceptors in the outer retina, which transduce the visual signal. Interneurons in the form of bipolar cells link the photoreceptors with ganglion cells, which convey the visual information to the brain. The photoreceptors are in close association with the retinal pigment epithelium (RPE) which performs many functions in maintaining the health of the retina. The retina is separated from the underlying vascular choroid by Bruch's membrane, damage to which is a feature of many retinal degenerative diseases. The high level of organisation into distinct layers is crucial to proper retinal function. Adapted from "Structure of the Retina", by BioRender.com (2023). Retrieved from https://app.biorender.com/biorender-templates

## 1.2 Age-related macular degeneration

AMD is a highly prevalent, acquired degenerative disease of the macula. It causes progressive impairment of the central vision, and in its end stages can result in a dense central scotoma which severely impairs vision-related functioning (Mitchell *et al.*, 2018). It is multifactorial in aetiology: age, genetic factors, uncontrolled oxidative stress, and inflammation are all thought to be central to its development (Ambati *et al.*, 2013). Typical clinical findings are abnormalities of the RPE and yellow subretinal deposits called drusen.

There are two main types of AMD, wet (neovascular) and dry (non-neovascular) based on the presence or absence of choroidal neovascularisation (CNV), with dry AMD representing 85-90% of cases. In dry AMD, our current treatment is limited to supplementation with carotenoids to slow progression (Sabour-Pickett *et al.*, 2014). There are more effective treatments for wet AMD in the form of intravitreal anti-VEGF therapies (Corazza *et al.*, 2021), but many patients still do not respond adequately (Krebs *et al.*, 2013) and there are potential serious complications associated with the available anti-VEGF therapies (Cox *et al.*, 2021).

The advanced stage of dry AMD is termed geographic atrophy, which is characterised by widespread loss of RPE and overlying photoreceptors, and resultant central visual loss. It is currently irreversible. Given the prevalence of dry AMD, its potential to cause irreversible damage to vision, and the current dearth of effective treatments, the study of this disease is of pressing concern.

### 1.3 AMD and the inflammatory response

There is clearly an immune component in the pathogenesis of AMD. The healthy retina is an immune-privileged site similar to the central nervous system, as it shows highly attenuated adaptive and innate immune responses (Forrester *et al.*, 2018). Several factors contribute to this, including a paucity of dendritic cells, tonic inhibitory signals present in the microenvironment, and the blood-retinal barriers (BRBs) (Guillonneau *et al.*, 2017). Thus in a state of health, mononuclear cells are normally excluded from the retina (Crane & Liversidge, 2008). However, studies in donor eyes with AMD show inflammatory cells – mononuclear cells and activated microglia – are present in the AMD retina (Gupta *et al.*, 2003; Lad *et al.*, 2015). In healthy eyes, the resident immune cell of the retina, the microglial cell, is inactive and generally confined to the inner retina, carrying out surveillance by continually sampling the retinal microenvironment (Diaz-Araya *et al.*, 1995; Lee *et al.*, 2008). However, in AMD, the microglia are activated and migrate to the subretinal space in areas of photoreceptor cell death (Gupta *et al.*, 2003). This migration appears to be a feature typical of most retinal degenerative disease (Guillonneau *et al.*, 2017).

Further evidence for the role of immune response in AMD comes from the presence of raised inflammatory cytokines, both systemically and in intraocular samples (Cao *et al.*, 2013; H. Miao *et al.*, 2012). Additionally, lifestyle factors that increase oxidative stress (eg smoking) increase the risk of developing AMD (Thornton *et al.*, 2005). Exactly which inflammatory pathways are involved in AMD pathogenesis is still under much discussion. One such pathway is mediated by inflammasomes.

### 1.4 The inflammasomes and pyroptosis

Inflammasomes are a group of multi-protein complexes activated by various pathways of the innate immune system, including in response to oxidative stress (Martinon *et al.*, 2009). In general, the components of the inflammasome complex are: a sensor – usually a nucleotide oligomerisation domain (NOD)-like receptor (NLR) or absent-in-melanoma (AIM)-2-like receptor (ALR); the adaptor molecule apoptosis-associated speck-like protein containing a CARD (ASC); and an effector enzyme, typically pro-caspase-1 (**Figure 1.2**).

Assembly of the inflammasome results in several downstream events with relevance to the inflammatory response (see further discussion below, section 1.5). Inflammasome activation can also trigger a distinct form of cell death called pyroptosis (Bergsbaken *et al.*, 2009). Pyroptosis is different from conventional apoptotic cell death in a number of respects. It is mediated by members of the gasdermin superfamily which form pores in the cell membrane and induce cell membrane lysis (Shi *et al.*, 2015). Both pyroptosis and conventional apoptosis involve DNA fragmentation, but in pyroptosis this occurs in the presence of an intact nucleus, as distinct from apoptosis (Jorgensen & Miao, 2015). The cell lysis observed in pyroptosis is also morphologically distinct from uncontrolled necrosis where explosive rupture of the cell is seen (Chen *et al.*, 2016).

The family of inflammasomes which were initially described are termed the canonical inflammasomes, but more recently a separate “non-canonical” inflammasome pathway has been investigated.

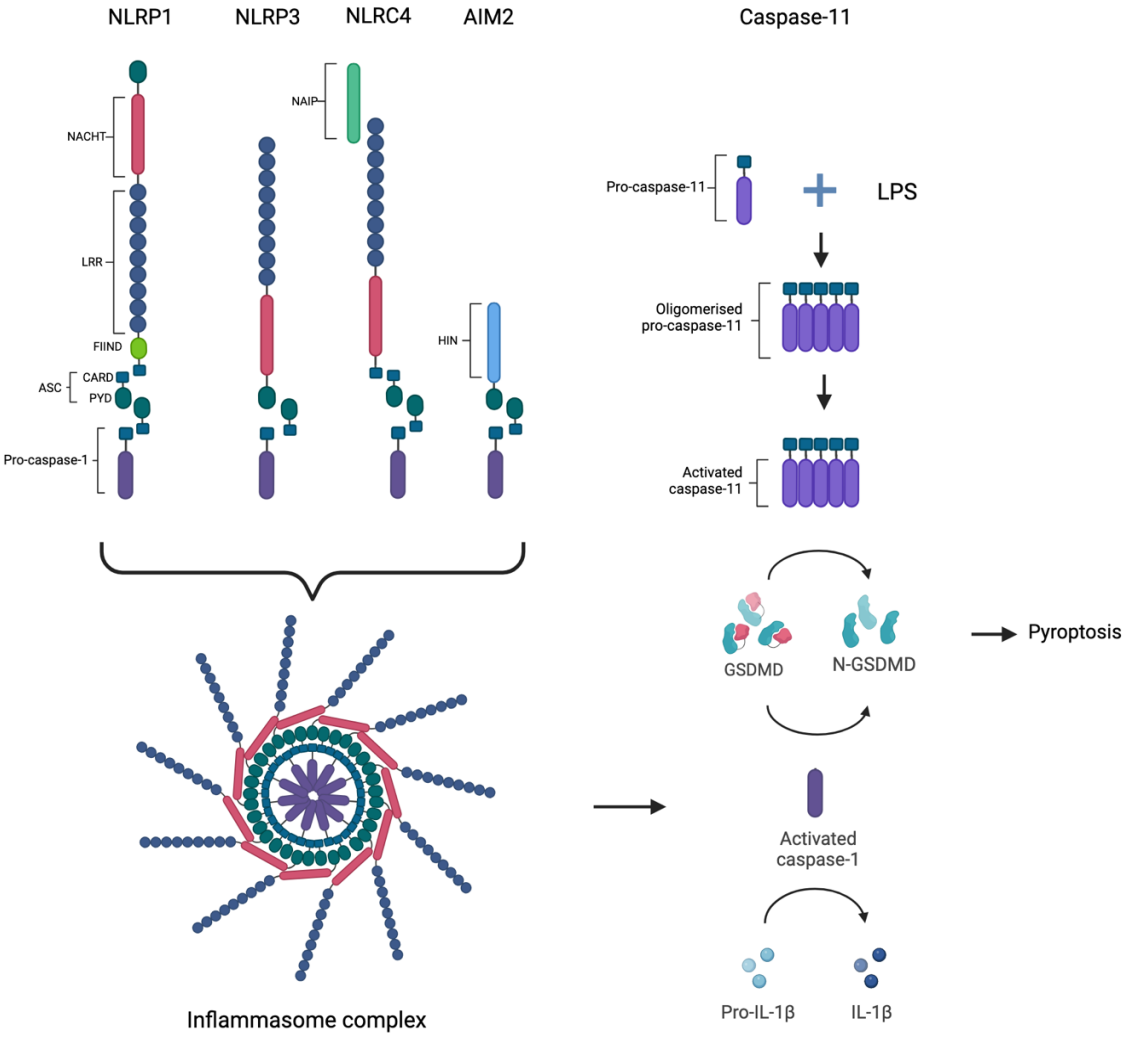


**Figure 1.2 The canonical and non-canonical inflammasomes.**

Sensor proteins (eg NLRP1, NLRP3, NLRC4, AIM2) form large complexes in response to damage or pathogens, called inflammasomes. These canonical inflammasomes use an adaptor protein ASC for their assembly. In contrast, caspase-11 can oligomerise (for example, via direct interaction with LPS) without requiring ASC. The assembly of canonical inflammasomes leads to downstream effects including cleavage of pro-IL-1β to its active form. Both activated caspase-1 and activated caspase-11 can process gasdermin D and induce pyroptosis. CARD = caspase activation and recruitment domain, FIIND = Function to find domain, GSDMD = gasdermin D, HIN = hematopoietic interferon-inducible nuclear protein domain, LPS = lipopolysaccharide, LRR = Leucine-rich repeat domain, N-GSDMD = Activated form of gasdermin D, NACHT = An NTPase domain present in NAIP, CIITA, HET-E, and TP-1, NAIP = NLR family apoptosis inhibitory protein, PYD = pyrin domain. Created with BioRender.com.

### 1.5 The canonical inflammasomes

The original and best-studied inflammasome is the NLRP3 inflammasome (Afonina *et al.*, 2017). NLRP3 is a pattern-recognition receptor (PRR) which is activated in response to a wide range of stimuli leading to the assembly of the inflammasome complex (Kelley *et al.*, 2019). One of the key features of the NLRP3 inflammasome and many others is the necessity of the ASC protein component as a "scaffold" molecule (Martinon *et al.*, 2002). Indeed, this molecule is common to all the canonical inflammasomes, and thus inhibiting ASC will block the assembly and activation of these inflammasomes.

Of the various sensor molecules in inflammasomes, the most well-studied are the NLRs. These are proteins that are found in the cytoplasm and can respond to cellular damage or pathogens. Not all NLRs are associated with inflammasome activation, but those that are with reasonable certainty include: NLRP1, NLRP3 (Martinon *et al.*, 2002), NLRP6 (Zheng *et al.*, 2021), NLRP7 (Khare *et al.*, 2012), NLRP12 (Vladimer *et al.*, 2012), and NLRC4 (Vance, 2015).

Another sensor that forms inflammasomes which is not of the NLR family is AIM2 (Hornung *et al.*, 2009). The evidence is less certain for IFN-γ inducible protein 16 (IFI16) (Kerur *et al.*, 2011), NLRP2 (Matsuoka *et al.*, 2019), and NLRC5 (Davis *et al.*, 2011). In ocular research the NLRP3 inflammasome has received the most attention, although other NLRs have been found to be expressed within the eye (Lim *et al.*, 2020).

Following assembly of the inflammasome, pro-caspase-1 is cleaved to its active form, caspase-1. Caspase-1 in turn converts pro-IL-1β to mature IL-1β, and pro-IL-18 to IL-18. IL-1β is the paradigm of a pro-inflammatory cytokine, performing various functions relating

to the inflammatory response including the promotion of further inflammatory mediators and increasing inflammatory cell migration (Dinarello, 2009).

The caspases in general are a family of proteases that are particularly associated with inflammation and cell death (Yi, 2020). Structurally, they have an amino-terminal domain and a protease domain. In caspases-1, -4, -5 and -11, the amino-terminal region contains a caspase recruitment domain (CARD), which is important in inflammasome assembly (Y. Li *et al.*, 2018; Smith & Creagh, 2022). Caspase activation can result in both pyroptosis and conventional apoptosis depending on the molecular context and which caspase is activated. Caspases-1, -4, -5, and -11 are all implicated in pyroptotic cell death (Shi *et al.*, 2015).

**1.6 The non-canonical Inflammasomes**

"Non-canonical" inflammasomes can act independently of the conventional caspase-1 pathway to result in pyroptosis. These are also not dependent on ASC for their function. They instead are formed by the oligomerisation of caspase-11 in the mouse or caspases-4/5 in the human (Kayagaki *et al.*, 2011). Caspase-11 is known to form inflammasomes in response to several pathogenic factors, the best-studied of which is cytosolic lipopolysaccharide (LPS) produced by Gram-negative bacteria in the context of sepsis (de Carvalho *et al.*, 2019; Gabrielli *et al.*, 2015; Shi *et al.*, 2014).

Similar to the canonical pathway, caspase-11 stimulates pyroptosis via interactions with gasdermin, leading to pore formation and rupture of the cell membrane (Kayagaki *et al.*, 2015). The in turn leads to passive release of inflammatory mediators, including IL-1$\beta$, from the intracellular compartment. While exogenous LPS is its most studied activator, a

role for caspase-11 has been proposed in a wide range of diseases, including the development of atherosclerosis (Jiang *et al.*, 2021), kidney injury (N. Miao *et al.*, 2019), and demyelinating disease (Hisahara *et al.*, 2001).

It is important also to note that some of the function of the non-canonical inflammasomes is mediated downstream by canonical inflammasomes, eg caspase-11 can subsequently activate the NLRP3 inflammasome during LPS transfection (Rühl & Broz, 2015). Much of this "cross-talk" between canonical and non-canonical inflammasomes has yet to be eludicated.

### 1.7 The Inflammasomes in AMD

Inflammasome dysregulation has been implicated in a wide range of inflammatory, neurodegenerative, and metabolic diseases (Guo *et al.*, 2015) and it is increasingly recognised that it has a role in the development of AMD in the eye. NLRP3 is present in the choroid and RPE of human eyes with geographic atrophy or neovascular AMD and localises to the site of lesions, but is not found in donor eyes of age-matched controls (Tseng *et al.*, 2013). The AMD retina additionally contains numerous activators of inflammasomes: lipid peroxidation product HNE (Kauppinen *et al.*, 2012), complement component C1Q, CEP (Doyle *et al.*, 2012), and amyloid-β (Dentchev *et al.*, 2003). The ASC protein component of the inflammasome was recently shown to be a biomarker for AMD (Weaver *et al.*, 2020).

Drusen components isolated from human donors with AMD were shown to upregulate NLRP3 in macrophages (Doyle *et al.*, 2012) and upregulated NLRP3 protein was also detected in the RPE of donor eyes (Tarallo *et al.*, 2012; Tseng *et al.*, 2013). In addition, the

disruption of lysosomes can trigger NLRP3 inflammasome activation in RPE cells – the lipofuscin component A2E which accumulates in AMD is known to have surfactant-like properties which can damage lysosomal membranes (Schütt *et al.*, 2002). Indeed, A2E can stimulate IL-1β release in ARPE cells via the NLRP3 inflammasome in ARPE cells (Anderson *et al.*, 2013).

However less is known about the role of caspase-11 in AMD. Caspase-4 (the human caspase-11 homolog) was found to be elevated in the RPE and choroid of human eyes with geographic atrophy (Kerur *et al.*, 2018). Oxidised phospholipids which are produced in damaged tissues can bind caspase-11 resulting in release of IL-1β (Zanoni *et al.*, 2016). Oxidised phospholipids accumulate in the retina with age and are particularly prevalent in AMD (Suzuki *et al.*, 2007). This is due to cumulative damage from oxidative stress.

**1.8 Oxidative stress**

One of the key areas of homeostasis in living organisms is the balance between pro- and anti-oxidant states. Oxidative stress is the condition where there is an predominance of oxidants over anti-oxidants (Sies *et al.*, 2017). Fundamental to oxidative stress is the production of reactive oxygen species (ROS), like the superoxide anion radical or the hydroxyl radical. Other reactive species involved in oxidative stress include reactive nitrogen species like nitric oxide, reactive sulphur species like cysteine and methionine, and reactive carbonyl species, such as various aldehydes.

Some oxidative stress is physiological, resulting in positive effects for the organism, one example being ischaemic tolerance (Yan, 2014). In addition, production of reactive oxygen species is one of the major components of the host defence against exogenous pathogens

(Thomas, 2017). However, excessive oxidative stress can have deleterious effects on tissues, leading to dysregulation or molecular damage. DNA oxidation is one of the major causes of genomic degradation, resulting in increased mutagenesis and potential oncogenesis (Cooke *et al.*, 2003). Proteins can be oxidised, which in some contexts can damage the function of the protein but in others can serve as a reversible modification supporting its signalling activities (Merker & Grune, 2000). The oxidation of lipids is seen in many diseases, including age-related macular degeneration (Mulfaul *et al.*, 2018).

Because excess oxidative stress is potentially so damaging, multiple strategies have been evolved to avoid or mitigate it. The presence of melanin in the retinal pigment epithelium is one such strategy, as it mitigates against photo-oxidative stress (Rozanowski *et al.*, 2008). A vast array of enzymes exist to reduce oxidants, including the superoxide dismutases, catalases, and glutathione peroxidases. When oxidative damage does occur, multiple systems exist to repair damaged molecules. These are often triggered within an inflammatory context (so-called “parainflammation”, or homeostatic inflammation). There are close links therefore between oxidative stress and the regulation of inflammation.

The damaging effects of oxidative stress are implicated in the pathogenesis of many conditions, including many retinal diseases.

### 1.9 Oxidative stress and the retina

The retina, even in health, must endure relatively high levels of oxidative stress, which is a corollary of its high metabolic demand and its function as light-sensitive tissue (Campochiaro & Mir, 2018; Kim *et al.*, 2021; Organisciak & Winkler, 1994). Oxidative

damage can result in the accumulation of waste products. Lipofuscin, which is a combination of oxidised protein and lipids, can often be seen clinically in degenerative retinal disease like AMD, although it also increases with age in the healthy eye (Delori *et al.*, 2001; Höhn & Grune, 2013). The RPE as it ages also shows other indicators of accumulating oxidative damage, like advanced glycation end-products (AGEs) (Handa *et al.*, 1999).

These waste products, as well as being present as a consequence of oxidative damage, can also play a role in producing it. For example, lipofuscin when it complexes with melanin and is exposed to blue light releases reactive oxygen species (Strauss, 2005).

The ongoing oxidative damage must be dealt with in some way if the tissue is to maintain its function. The notion of "parainflammation", or a homeostatic inflammatory response, has been proposed as one way that the retina can clear oxidative waste products (H. Xu *et al.*, 2009). For example, in AMD, macrophages are often seen to accumulate around drusen, and it has been suggested that these may serve to prevent further growth of drusen (Guillonneau *et al.*, 2017). One theory of age-related disease is that this beneficial parainflammatory response becomes dysregulated in some respect, leading to chronic low-grade inflammation and tissue damage (Medzhitov, 2008).

### 1.10 Mouse models used in study of AMD

While ideally we would like to study mechanisms of disease in human subjects, this is usually not practical or ethically viable. Animal models provide a convenient alternative. There are a wide range of mouse models which have been used as a surrogate for the

human disease of AMD, each with their own advantages and disadvantages. Our model, the sodium iodate model, is one of the earliest described that is still in use.

In general in mouse models of AMD, retinal damage is induced by various methods, most commonly chemically (as in sodium iodate) or using a genetic variant. An alternative is the photo-oxidative model of retinal degeneration, in which light exposure damages the retina due to increased oxidative stress (Natoli *et al.*, 2016). One advantage of this model is that chronic damage can be induced by exposure over a number of days, which is closer to the chronic nature of AMD than many chemical models where damage is induced by a single, acute exposure. However, the association between light exposure and the development of AMD is controversial (Zhou *et al.*, 2018), and is certainly not the predominant mechanism of injury in that disease.

Given the importance of oxidative stress in the development of retinal degeneration, it is logical that animals with defects in anti-oxidative processes may develop a degenerative phenotype. This is the case with *Sod1* knockout mice, which lack copper/zinc superoxide dismutase, and develop drusen-like deposits and a thickened Bruch's membrane with ageing (Imamura *et al.*, 2006). A similar enzyme, manganese superoxide dismutase (MnSOD) which converts superoxide to hydrogen peroxidase is encoded by *Sod2*. Unfortunately, complete knockout of *Sod2* is invariably fatal (Y. Li *et al.*, 1995) so alternative strategies have been used to selectively knockout *Sod2* within tissues of interest. Using an adeno-associated virus (AAV), it is possible to deliver a ribozyme that cleaves the mRNA for MnSOD specifically within the RPE (Justilien *et al.*, 2007). This leads to retinal degeneration with similarities to the AMD phenotype. This technique was subsequently altered to delete *Sod2* using a cre/lox system with similar results (H. Mao *et*

*al.*, 2014). These techniques require additional expertise and add further levels of complication when compared with, for example, a single administration of a chemical agent.

We know that certain genetic variants increase the risk of the development of AMD, one of which is complement factor H (Cfh). It therefore made conceptual sense to explore the phenotype of Cfh-deficient mice. While these mice do have photoreceptor dysfunction and decreased vision, this is in the context of constant activation of the alternative complement pathway and continuous high-level consumption of C3, which is not seen in AMD (Coffey *et al.*, 2007). An alternative model was developed using Cfh transgenic mice that express chimeric Cfh molecules which are ineffective in the retina while still being functional in other contexts (Ufret-Vincenty *et al.*, 2010). These mice, when subject to oxidative stressors, including ageing, develop increased basal laminar deposits which can also be seen in AMD (Aredo *et al.*, 2015).

Mice deficient in Ccl2, a chemokine involved in the chemotaxis of monocytes, develop many features of AMD, including drusen, photoreceptor atrophy, and choroidal neovascularisation (Ambati *et al.*, 2003). RPE cells express Ccl2 in response to inflammation and oxidative stress (Higgins *et al.*, 2003) and dysfunction of Ccl2 may be involved in the accumulation of monocytes and microglial cells in the subretinal space in various pathologies (Raoul *et al.*, 2010). Another molecule which has been associated with AMD via a single nucleotide polymorphism is CX3CR1, a chemokine receptor (Tuo *et al.*, 2004). *Cx3cr1*-deficient mice are apparently normal with respect to ocular health. However, the double knockout $Ccl2^{-/-}/Cx3cr1^{-/-}$ mouse developed the AMD phenotype without the ageing required in $Ccl2^{-/-}$ mice (Tuo *et al.*, 2007). The

caeruloplasmin/hephaestin double knockout mouse (*Cp*$^{-/-}$*Heph*$^{-/-}$) similarly is reported to display many AMD features (Hahn *et al.*, 2004).

Neovascular AMD is quite a different disease in terms of pathogenesis, and its mouse models are reviewed elsewhere (Rastoin *et al.*, 2020).

### 1.11 The sodium iodate model

Sodium iodate ($NaIO_3$) is a potent oxidising agent, and when it is administered systemically in animal models it is toxic to the retina (Carido *et al.*, 2014; Franco *et al.*, 2009; Hanus *et al.*, 2016; Noell, 1953; Sorsby, 1941). While the exact sequence of pathogenic events remains to be clarified, most agree that sodium iodate causes impairment of the RPE first, leading to RPE atrophy and subsequent photoreceptor degeneration in the subjacent outer nuclear layer (W. Wang *et al.*, 2011). It was suggested several decades ago that part of the toxicity of sodium iodate to the RPE is due to its effect on melanin by increasing the melanin's ability to convert glycine to glyoxylate (Baich & Ziegler, 1992).

Whether sodium iodate produces temporary or permanent damage varies according to the dosage; in general lower doses produce a reversible effect, while larger doses result in structural damage with irreversible loss of photoreceptors (Enzbrenner *et al.*, 2021).

There is accumulating evidence for inflammasome activation in sodium iodate injury. For example, mRNA of il-1β was found to be increased in the retina of the sodium iodate mouse (Enzbrenner *et al.*, 2021). In ARPE-19 cells, NLRP3 was activated by sodium iodate, and the use of mesenchymal stem cells to inhibit NLRP3 led to increased cell survival (X. Mao *et al.*, 2018). The relevance of caspases to this process was demonstrated using a

transfected form of the caspase activation and recruitment domain (CARD) in sodium iodate injury (Young *et al.*, 2019). There was increased functional recovery by using this CARD to bind caspase-1 preventing its activation.

The mouse is the most common animal used in these experiments at present, due to the relative ease of studying the effect of sodium iodate in wild-type and genetic knock-out strains (Hinton & Kannan, 2014). The retinal lesions induced by sodium iodate in the mouse share many similarities with the atrophic lesions of dry AMD.

**1.12 Mechanisms of cell death in the sodium iodate model**

As is the case in AMD itself, it is controversial which cell death mechanisms are operative in the sodium iodate model. In AMD, Hageman *et al*. (2001) considered necrosis the most likely candidate for RPE cells, based on the histopathological work available at that time, and also based on the recruitment of leukocytes, which is often not seen with standard apoptotic cell death. Necrosis is an uncontrolled form of cell death involving cell membrane rupture and cell lysis in response to injury (Berghe *et al.*, 2010). While necrosis has previously been considered an unregulated and passive form of cell death, it is increasingly recognised that at least some of what we consider necrosis is in fact programmed cell death, and this has been termed necroptosis (Christofferson & Yuan, 2010).

Sodium iodate certainly has a damaging effect on RPE cells, but it is not settled whether most of the RPE cells in the sodium iodate model die by necrosis/necroptosis, or another form of cell death. Kaneko *et al*. (2011) found evidence of caspase-3 cleavage in the RPE of donor eyes with geographic atrophy, but not in control eyes, which suggests that

caspase-dependent pathways are at play in the disease. More recently, pyroptosis via inflammasomes has been implicated (Tarallo *et al.*, 2012).

Additionally, the contribution of the photoreceptors has not been fully elucidated: do the photoreceptors die secondarily as a result of RPE loss, or do they undergo cell death as a direct result of sodium iodate toxicity? And if so, what form of cell death do they undergo?

The identification of necrotic cell death to the exclusion of other forms of cell death can be difficult. The widely used TUNEL assay is not specific to one type of cell death, as it relies on the detection of free DNA ends, which are present in several forms of cell death. Balmer *et al*. (2015) used the rupture of the cell membrane combined with the absence of caspase-3 activity, as assessed by the ApoToxGlo assay, as a marker of necrosis in sodium iodate injury.

The ARPE-19 cell line (a widely used human RPE cell line) when exposed to oxidative stress with sodium iodate did not show typical features of apoptosis, including DNA chromatin condensation, DNA fragmentation, and caspase-3 activation (Hanus *et al.*, 2013, 2016). In contrast, rapid ATP depletion was seen, which is more consistent with necrosis (or necroptosis) as opposed to apoptosis. In addition, necrosis inhibitors, but not a pan-caspase inhibitor, increased ARPE-19 survival.

This *in vitro* work in ARPE-19 cells can be supplemented with that of Balmer *et al*. (2015) and J. Wang *et al*. (2014). Balmer *et al*. (2015) isolated primary mouse RPE cells for testing with sodium iodate, and they also used a murine cone-like photoreceptor cell line 661W. They report necrosis is the primary cell death response in RPE cells, while 661W cells instead underwent caspase-dependent cell death. Similarly, J. Wang *et al*. (2014) showed

that 661W cells die in a dose-dependent manner in response to sodium iodate associated with an increase in ROS production.

RIPK3 is a molecule essential to the formation of the necrosome, which is an aggregate of microfilament-like complexes required for necroptosis (J. Li *et al.*, 2012). RIPK3 aggregation and activation has been associated with NLRP3 inflammasome activation (Lawlor *et al.*, 2015), so it might be hypothesised that the NLRP3 inflammasome is active in this model. However, *in vitro* studies did not detected canonical inflammasome formation (by ASC-GFP) and additionally a caspase-1 inhibitor did not protect the ARPE-19 cells (Hanus *et al.*, 2016). This does not, however, exclude a contribution from non-canonical inflammasomes.

In contrast to this work, X. Mao *et al*. (2018) did find an increase in NLRP3, caspase-1, and IL-1β in ARPE-19 cells treated with sodium iodate, implicating inflammasomes and pyroptosis. Recent work by our lab has shown an important role for Sarm1 (sterile alpha and armadillo motif-containing protein), a Toll/IL-1 receptor (TIR) adaptor, in sodium iodate-induced photoreceptor cell death (Gibbons *et al.*, 2022; Ozaki *et al.*, 2020). We know from other contexts that Sarm1 has a role in promoting degeneration of axons in neuronal injury (Osterloh *et al.*, 2012), and likewise blocking Sarm1 appears to be protective from the retinal damage of oxidative stress. The exact mechanism behind this is not clear but blocking Sarm1 in macrophages reduces inflammasome-related pyroptosis (Carty *et al.*, 2019) and this may also be also be relevant in this model.

In summary, while there is extensive evidence for inflammation in AMD, the role of the inflammasome and the relative contribution of the canonical and non-canonical pathways

has yet to be established. The sodium iodate model provides a useful tool for examining retinal damage in this context. We proposed to examine the sodium iodate model in two genetic knock-out mice, *Pycard*$^{-/-}$ and *Casp11*$^{-/-}$ mice, the former lacking the ability to assemble canonical inflammasomes, while the latter are unable to form non-canonical inflammasomes. In this way we hoped to further clarify the contributions of the various inflammasomes in the sodium iodate mouse.

**1.13 Aims and objectives**

1. Perform a comprehensive review of the literature of inflammasomes in retinal degeneration (published as Silke *et al*., 2023)

2. Compare the retinal degeneration induced by sodium iodate over time in ASC knock-out and wild-type mice, in terms of

(a) histological features of retinal and RPE damage

(b) *in vivo* measurements of damage with OCT, and

(c) levels of cell death via immunofluorescence (TUNEL staining)

3. Compare the retinal degeneration induced by sodium iodate over time in caspase-11 knock-out and wild-type mice, in terms of

(a) histological features of retinal and RPE damage

(b) *in vivo* measurements of damage with OCT, and

(c) levels of cell death via immunofluorescence (TUNEL staining)

# 2. Materials and Methods

## 2.1 Mice

Three groups of mice were used in these experiments, C57BL/6J, *Pycard*$^{-/-}$, and *Casp11*$^{-/-}$, all 8-12 weeks old. Mice were housed in a standard laboratory environment with a twelve-hour light-dark cycle at 21 degrees Celsius in the Ocular Genetics Unit in Trinity College Dublin (TCD), with access to food and water *ad libitum*. The experiments were approved by an internal ethics committee in TCD, and all procedures were performed in accordance with the regulations in the ARVO Statement for the Use of Animals in Ophthalmic and Vision Research. The Health Products Regulatory Authority (HPRA) authorisation number for the project was AE19136/P104.

In the first set of experiments, wild-type and *Pycard*$^{-/-}$ mice were compared. The specific numbers and sex distribution of the mice at the various timepoints were as follows: Day 1 wild-type n=5 (all female); day 1 *Pycard*$^{-/-}$ n=6 (three female, three male); day 2 wild-type n=4 (two male, two female); day 2 *Pycard*$^{-/-}$ n=6 (three male, three female); day 7 wild-type n=5 (one male, four female); day 7 *Pycard*$^{-/-}$ n=6 (four female, two male).

For the subsequent experiments in *Casp11*$^{-/-}$ mice, the timepoints were changed to day 3 and day 7, and all mice were female (see discussion section for the reasoning behind these changes). For these experiments, the n for all groups was 4. The exception to this is the TUNEL experiment in *Casp11*$^{-/-}$ mice which was performed prior to these changes. For this experiment, the numbers and sex distribution of the mice were as follows: Day 2 wild-type n=4 (two male, two female); day 2 *Casp11*$^{-/-}$ n=5 (four male, one female); day 7 wild-type n=3 (three female); day 7 *Casp11*$^{-/-}$ n=4 (three female, one male).

## 2.2 Sodium iodate model

We administered a sterile solution of $NaIO_3$ as a single intraperitoneal injection (70mg/kg body weight) to study mice. Control mice received normal saline. The mice were euthanised at the relevant timepoint by cervical dislocation. Both eyes were enucleated. Eyes for paraffin sections were fixed in Davidson's fixative overnight (see section 2.9.2 for composition). Eyes for cryosections underwent lens extraction under a microscope and were then fixed in 4% paraformaldehyde (section 2.9.3) for 1.5 hours.

## 2.3 OCT

Mice for optical coherence tomography (OCT) were given a single intraperitoneal injection of medetomidine (10mg/kg) and ketamine (50mg/kg) to induce chemical restraint. Their pupils were dilated with topical tropicamide 1% and phenylephrine 2.5%. OCT images were taken of each eye at the central retina and at the temporal and nasal periphery. The mice were then given an intraperitoneal injection of atipamezole (1mg/kg) to reverse chemical restraint, and were placed in a heated chamber to recover. The thickness of the outer nuclear layer (ONL) was measured in ImageJ and averaged across the three areas sampled.

## 2.4 Paraffin embedding

The fixed eyes were washed in phosphate-buffered saline (PBS, section 2.9.1) three times before being placed in tissue embedding cassettes (Sigma-Aldrich) and submerged in 80% ethanol. A tissue processor (Leica) was used to dehydrate the eyes. Under gentle agitation, the tissue was exposed to 70% ethanol for 1 hours, 80% ethanol for 1 hour, 95%

ethanol for 1 hour, 100% ethanol for 1 hour twice, 50% ethanol/xylene for 1 hour, xylene for 1 hour twice, and paraffin at 60 degrees Celsius for 1 hour. The tissues were removed from the cassettes and a paraffin embedding system (Leica) used to embed them in paraffin wax. A microtome (Leica) was used to cut 5μm sections of the tissue. The sections were floated on a water bath at 50 degrees Celsius to flatten them and placed onto slides coated with polylysine (Fisher Scientific). The slides were left to dry overnight at room temperature.

**2.5 Cryosectioning**

Paraformaldehyde-fixed eyes were washed thoroughly with PBS. The eyes were cryopreserved by placing in a 20% sucrose solution for one hour and then 30% sucrose overnight at 4 degrees Celsius. Optimal cutting temperature (OCT) compound (Fisher Scientific) was used to embed the tissue. The tissue was frozen with liquid nitrogen. A Leica CM1900 cryostat was used to cut 12μm sections, which were collected on polylysine-coated slides (Fisher Scientific) and stored at 4 degrees Celsius.

**2.6 Haematoxylin and eosin (H+E) staining**

Paraffin slides were deparaffinised with xylene, and then rehydrated with ethanol by dipping 10 times in 100% ethanol, 10 times in 90% ethanol, then 10 times in 70% ethanol. The slides were exposed to haematoxylin (Sigma Aldrich) for 6 minutes, and then the stain was washed thoroughly with water. Eosin (Sigma Aldrich) was then applied for 3 minutes, followed by a further wash. Dehydration of the slides proceeded as followed: 10 dips in 70% ethanol, 10 in 90% ethanol, 10 in 100% ethanol, and 20 dips in xylene. The slides were mounted with mounting medium (Sub-X®, Leica Biosystems). Photomicrographs were

taken at 4x, 20x and 40x power (Leica DMLB light microscope). Three 40x photomicrographs per slide and two slides from the central part of the eye per eye were selected for analysis, using Image J. The selected slides were taken from approximately the same retinal area by taking the same slide number in each mouse. The number of outer nuclear layer (ONL) photoreceptor nuclei were counted within a 450 pixel square at the centre of the slide, and an average per mouse calculated. In a similar manner, the number of rows in the ONL was measured. The number of breaks in the RPE monolayer was counted for each slide and an average per mouse obtained. To calculate the area of RPE, the RPE was bounded by freehand selection and the number of pixels within the selection was recorded (all 40X images had a standard size of 1600x1200 pixels).

**2.7 TUNEL staining**

To perform terminal deoxynucleotidyl transferase dUTP nick end labelling (TUNEL) staining, the tissue sections were rehydrated as previously described. They were then permeabilised by covering for 8 minutes with a mixture of 0.1% Triton and 0.1% sodium citrate. This was then washed off with three washes of PBS. The reagents from the *In Situ* Cell Death Detection Kit, TMR red Protocol (Roche) were combined in accordance with the manufacturer's protocol to form the reaction mixture. 50μm of the reaction mixture was placed on each slide, and the slides were placed in a humidified chamber for 1 hour at 37 degrees Celsius. Following a further three washes with PBS, the slides were mounted with Mowiol 4-88 (Sigma-Aldrich). Photomicrographs of the stained slides were taken with a Zeiss LSM 700 confocal microscope. Eight images were taken per slide to capture the entire retinal section, and TUNEL-positive cells were counted using Image J.

### 2.8 Statistical analysis

Values between groups of mice were compared using a two-tailed Student's t-test within GraphPad Prism (San Diego, CA), with a p-value of <0.05 considered significant. The results were graphed displaying mean $\pm$ standard deviation.

### 2.9 Materials

#### 2.9.1 Phosphate Buffered Saline (PBS)

A stock 10x solution of PBS was made in the following manner: The reagents sodium chloride NaCl (80g), potassium chloride KCl (2g), disodium phosphate $Na_2HPO_4$ (14.4g), monopotassium phosphate $KH_2PO4$ (2.4g) were dissolved in 800mL of distilled $H_2O$. Concentrated hydrochloric acid (HCl) was added to adjust the pH of the solution to 7.4 as measured by a pH meter. Finally, the solution was made up to 1000mL with distilled $H_2O$.

As needed, 100mL of this stock solution was diluted with a further 900mL distilled $H_2O$ to produce a 1x solution.

#### 2.9.2 Davidson's fixative

This fixative was made by combining: 300mL of 95% ethanol, 200mL of 10% neutral buffered formalin, 100mL of anhydrous acetic acid, and 300mL of distilled $H_2O$.

#### 2.9.3 4% paraformaldehyde

To make a 4% paraformaldehyde solution, 4g of paraformaldehyde were added to 50mL of distilled H2O. 1mL of 1M NaOH was added to this solution. The solution was heated at 60 degrees Celsius, stirring until the paraformaldehyde completely dissolved. 10mL of 10x

PBS were added and the mixture was allowed to cool to room temperature. The pH of the solution was adjusted to 7.4 with HCl (usually about 1mL of 1M HCl). The solution was made up to 100mL with $H_2O$. The solution was filtered through a 0.45μm membrane to remove any particulate matter. The solution was stored in aliquots at -20 degrees Celsius.

# 3. Results

## 3.1 Histological analysis indicates ASC deficiency does not protect against RPE fragmentation in the sodium iodate model of retinal degeneration

Sodium iodate is primarily known to cause acute degeneration of the RPE. For this reason we initially examined the integrity of the RPE monolayer by H&E of wild-type and *Pycard*$^{-/-}$ mice at day 1, day 2, and day 7 following administration of sodium iodate (**Figure 3.1**).

At baseline, no differences were evident at the level of the RPE between wild-type and *Pycard*$^{-/-}$ mice, with a continuous monolayer of RPE cells present and healthy nuclei visible. At day 1, this monolayer is mostly still preserved in both groups, with occasional disruptions. Several of the RPE nuclei can be seen in various stages of dissolution. By day 2, multiple discontinuities appear in the RPE layer although the RPE is still clearly identifiable. Outpouchings of the RPE are seen to develop, suggesting inward migration of RPE cells towards the retina. By day 7, there is complete breakdown of the RPE structure. Gross histological differences in RPE structure were not observed between the wild-type and *Pycard*$^{-/-}$ mice at any timepoint. The number of RPE breaks induced by sodium iodate was similar between the two groups of mice at all timepoints and there were no differences in the total area of RPE, suggesting thinning and loss of RPE was occurring at equal rates in both genotypes (**Figure 3.1B**).

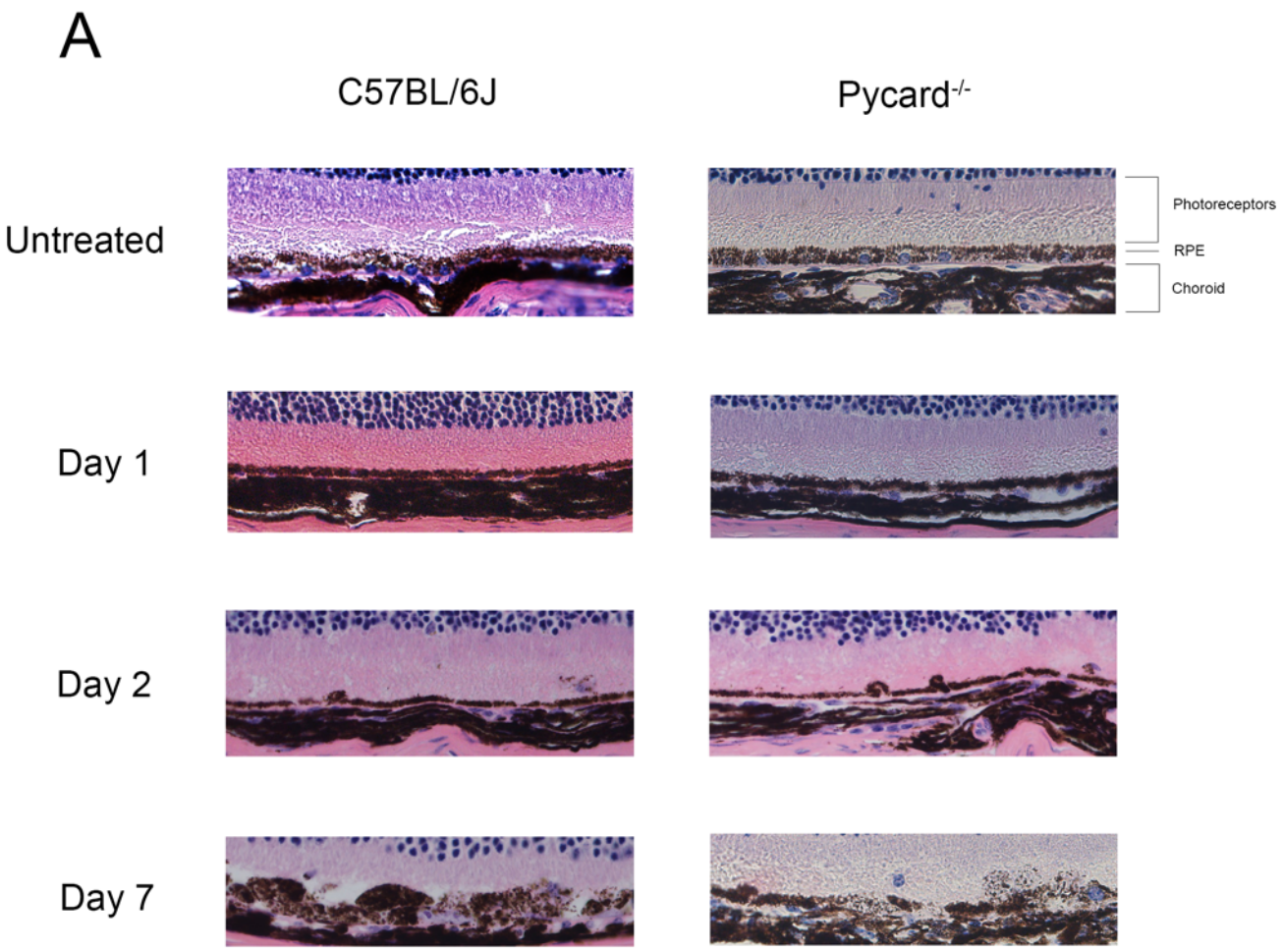


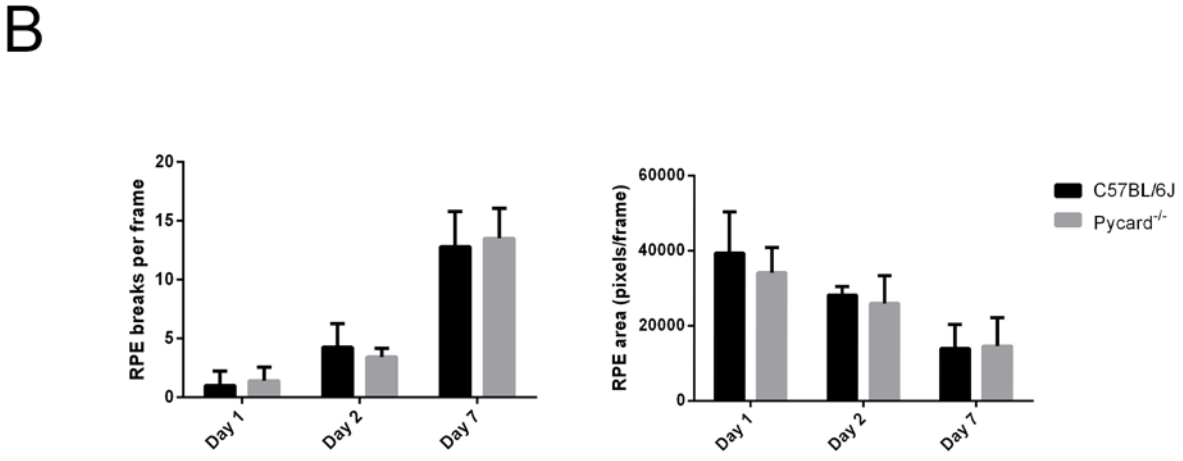


**Figure 3.1 Histology of retinal pigment epithelium (RPE) in wt and *Pycard*$^{-/-}$ mice**

Central and peripheral areas of H&E stained RPE in wt and *Pycard*$^{-/-}$ mice were imaged at 40X magnification and the number of RPE breaks counted and RPE area measured. Day 1 wt n=5 (all female), *Pycard*$^{-/-}$ n=6 (three female, three male); day 2 wt n=4 (two male, two female), *Pycard*$^{-/-}$ n=6 (three male, three female); day 7 wt n=5 (one male, four female), *Pycard*$^{-/-}$ n=6 (four female, two male) [A] Representative images at baseline and at days 1, 2 and 7 following administration of sodium iodate. [B] There was no difference in the number of RPE breaks or total RPE area at any timepoint (graph shows mean ± SD of the average of two central sections

### 3.2 Histological analysis indicates ASC deficiency does not protect against loss of photoreceptors in the sodium iodate model of retinal degeneration

Loss of RPE impacts the health of the photoreceptors, however our lab has previously observed that despite RPE degeneration occurring in Sarm deficient mice apace with wild-type mice, that photoreceptors were protected from acute degeneration (Gibbons *et al.*, 2022). We therefore next investigated the effect ASC deficiency had on photoreceptor degeneration (**Figure 3.2**).

At baseline, there were no ultrastructural differences between wild-type and *Pycard*$^{-/-}$ mice. The photoreceptor layer is seen to be highly organised with a clear distinction between the photoreceptor inner and outer segments. This distinction largely persists at day 1 following administration of sodium iodate, with preservation of the photoreceptor nuclei in the outer nuclear layer. However at day 2, we begin to lose the separation between the photoreceptor inner and outer segments as the outer retina becomes more disorganised. This is accompanied by a reduction in the number of photoreceptor nuclei and a loss of thickness of the ONL. By day 7, the photoreceptor layer has become very thin and in some areas completely obliterated. This loss of photoreceptors is accompanied by attenuation of the ONL.

We quantified the outer nuclear layer in the groups by two methods, and we were unable to identify any difference with respect to preservation of photoreceptor nuclei (**Figure 3.2B**).

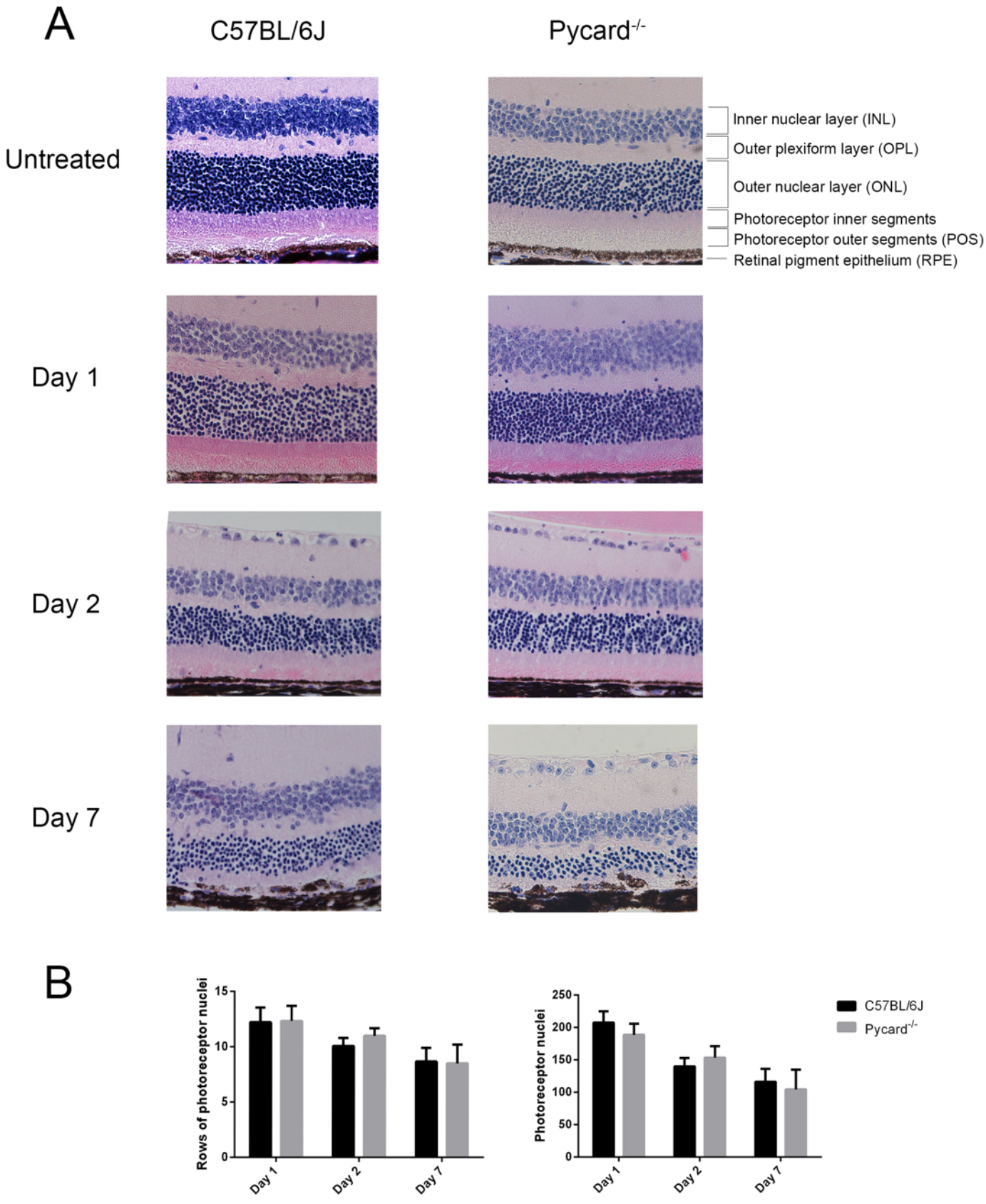


**Figure 3.2 Histology of outer nuclear layer (ONL) in wt and *Pycard*$^{-/-}$ mice**

Central and peripheral areas of H&E stained retinas in wt and *Pycard*$^{-/-}$ mice were imaged at 40X magnification and the photoreceptor nuclei in outer nuclear layer (ONL) were quantified. Day 1 wt n=5 (all female), *Pycard*$^{-/-}$ n=6 (three female, three male); day 2 wt n=4 (two male, two female), *Pycard*$^{-/-}$ n=6 (three male, three female); day 7 wt n=5 (one male, four female), *Pycard*$^{-/-}$ n=6 (four female, two male) [A] Representative images at days 1, 2 and 7 following administration of sodium iodate. [B] Quantification of photoreceptor nuclei density in outer nuclear layer from two central retinal sections per mouse averaged (mean ± SD).

### 3.3 Optical coherence tomography indicates ASC deficiency does not protect against loss of photoreceptors in the sodium iodate model of retinal degeneration

We next wanted to confirm that our histological findings correlated with *in vivo* measurements. Optical coherence tomography (OCT) provides *in vivo* cross-sectional imaging of the retina, and allows quantification of retinal layer thickness in the living mouse. We performed OCT imaging at baseline and at day 7 following administration of sodium iodate in wild-type and *Pycard*$^{-/-}$ mice (**Figure 3.3**). Thinning of the ONL was seen in all mice at day 7, with no difference between mice with and without Asc protein (**Figure 3.3B**).

### 3.4. Quantification of cell death by TUNEL staining indicates photoreceptors are degenerating at the same rate in both wild-type and ASC-deficient mice

The death of photoreceptors is one of the key pathological events in sodium toxicity which results in visual loss. We used TUNEL staining on retinal sections at day 2 and day 7 to assess the timing and extent of cell death in *Pycard*$^{-/-}$ and wild-type mice (**Figure 3.4**). Strong TUNEL staining was seen at day 2 in both groups of mice, indicating brisk cell death occurring at this timepoint. By day 7, only minimal TUNEL staining is apparent, suggesting that the majority of cell death has taken place before this point. We quantified the amount of TUNEL staining by counting the TUNEL positive cells in the ONL (**Figure 3.4B**). There was no difference between the two groups at either timepoint, indicating that the death of photoreceptors is occurring at a similar rate.

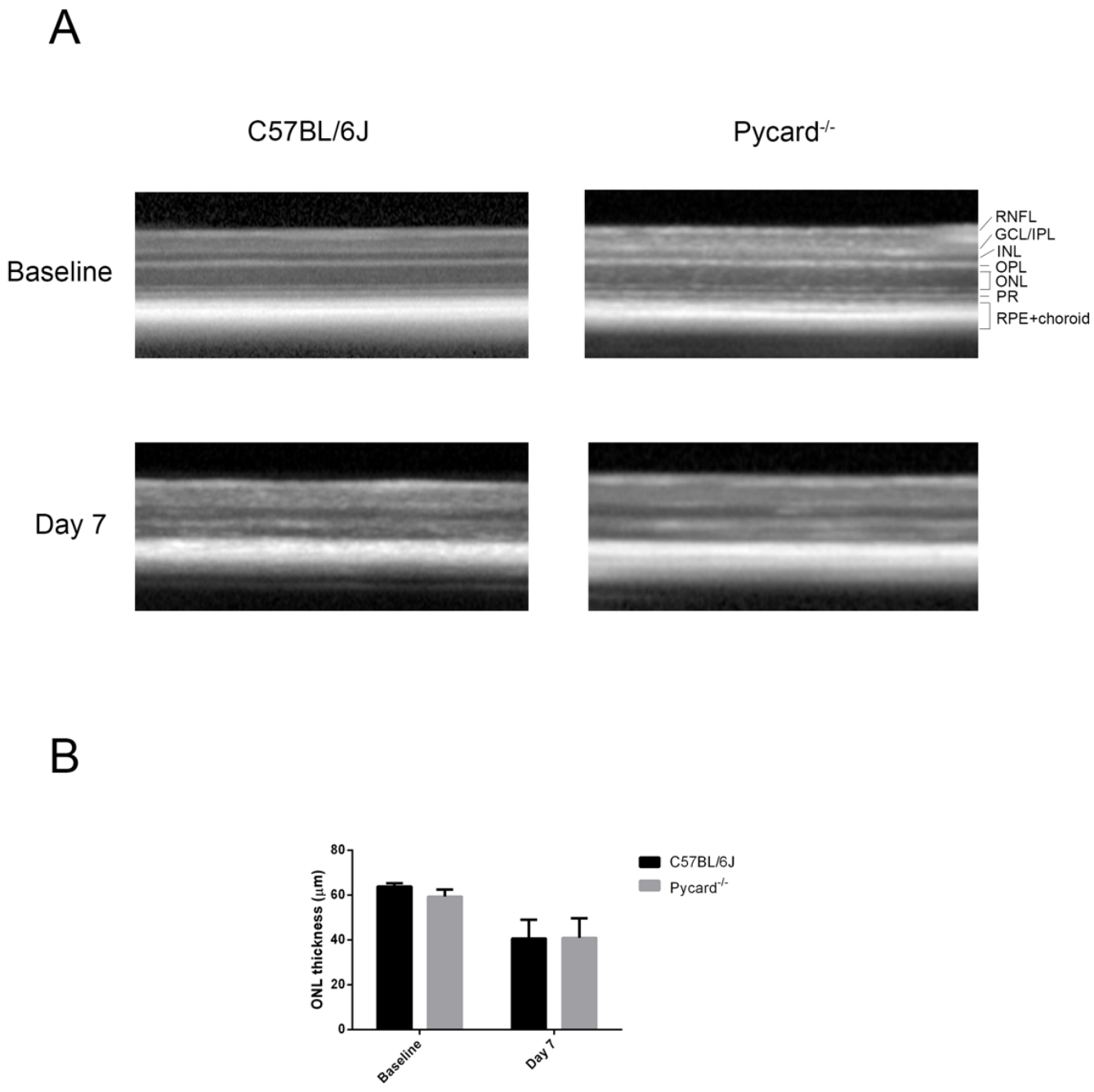


**Figure 3.3 Retinal ONL thickness by OCT in wt and *Pycard*$^{-/-}$ mice**

Cross-sectional *in vivo* OCT images of the posterior pole and nasal and temporal retina in wild-type C57BL/6J mice and *Pycard*$^{-/-}$ mice were taken, with measurement of outer nuclear layer (ONL) thickness. wt n=5 (one male, four female), *Pycard*$^{-/-}$ n=6 (four female, two male) [A] Representative images at baseline (immediately preceding intervention) and on day 7 following administration of sodium iodate. [B] Bar diagram shows mean ONL thickness as an average of the three regions sampled ± SD. The results were not significant.

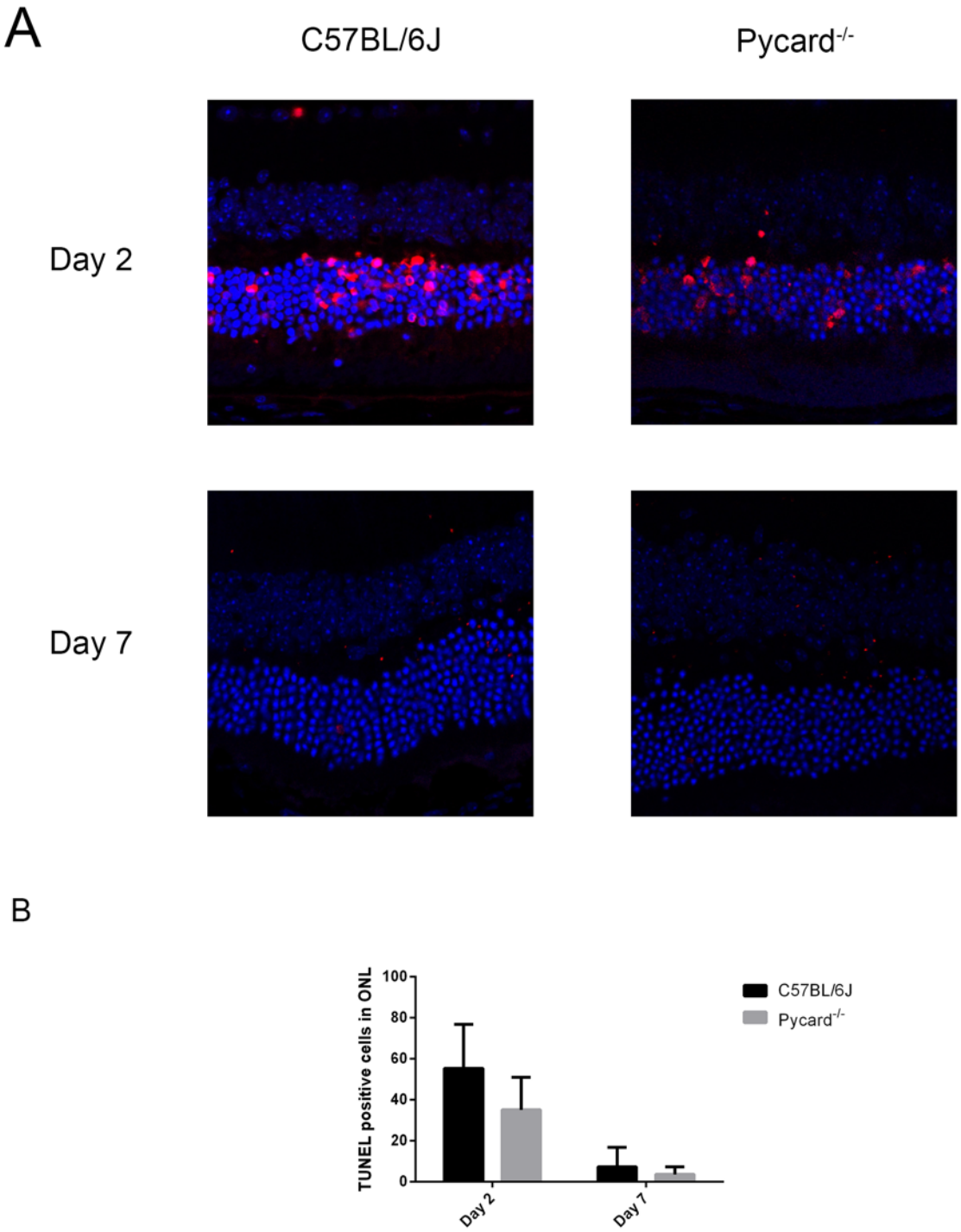


**Figure 3.4 TUNEL staining the ONL in wt and *Pycard*$^{-/-}$ mice**

TUNEL-stained central retinal tissue sections of wild-type and *Pycard*$^{-/-}$ mice were imaged at 40X and number of TUNEL-positive cells in the ONL were measured. Day 2 wt n=4 (two male, two female), *Pycard*$^{-/-}$ n=6 (three male, three female); day 7 wt n=5 (one male, four female), *Pycard*$^{-/-}$ n=6 (four female, two male) [A] Representative images on day 2 and day 7 following administration of sodium iodate. [B] Bar diagram shows number of TUNEL positive cells. Results are an average of eight images across a single central section. Error bars represent mean ± SD. The results were not significant at any timepoint.

### 3.5 Histological analysis indicates caspase-11 deficiency does not protect against RPE fragmentation in the sodium iodate model of retinal degeneration

By blocking ASC, we effectively excluded any contribution of the canonical inflammasome pathway to the degeneration of RPE or photoreceptors in sodium iodate injury. We next investigated the non-canonical inflammasome pathway with caspase-11-deficient mice (**Figure 3.5**).

We compared the RPE of *Casp11*$^{-/-}$ mice to wild-type mice at day 3 and 7 following sodium iodate administration by histological analysis. At baseline, there were no differences seen at the level of the RPE between the two genotypes. A healthy continuous monolayer of RPE was visible in all mice. At day 3, multiple discontinuities in the RPE are seen, with areas of intraretinal migration similar to that seen at the intermediate time-point in the *Pycard*$^{-/-}$ mouse. By day 7, the RPE is completely disrupted and large melanin-loaded cells are present. The spectrum of histological damage to the RPE seen over time was similar to that observed in the *Pycard*$^{-/-}$ experiment. We were unable to identify any differences between the RPE of wild-type and *Casp11*$^{-/-}$ mice at any timepoint. The amount of induced RPE breaks at a histological level were similar between the two groups as was the total RPE area (**Figure 3.5B**).

### 3.6 Histological analysis indicates caspase-11 deficiency may protect against loss of photoreceptors in the sodium iodate model of retinal degeneration

As the damage to RPE appeared similar in caspase-11 and wild-type mice, we would expect similar findings in the photoreceptor layer, if the loss of photoreceptors in the sodium iodate model is primarily due to the RPE degeneration. To investigate this, we

next examined the photoreceptor layer in *Casp11*$^{-/-}$ and wild-type mice following sodium iodate administration (**Figure 3.6**).

At baseline, no differences between the two genotypes were seen. By day 3 following sodium iodate administration, the number of photoreceptor nuclei in the ONL could be seen to be reduced. Accompanying this was disorganisation of the photoreceptors, with loss of a clear inner segment-outer segment junction. By day 7, the photoreceptor layer is markedly thinned along with the ONL, with absence of photoreceptors in many areas. However, the loss of photoreceptors appeared to be somewhat less in the *Casp11*$^{-/-}$ mice. We quantified this using the same methods as in the previous experiments. There was a definite trend towards a protective effect in the *Casp11*$^{-/-}$ mice as more photoreceptor nuclei survived at both day 3 and day 7. This effect however did not meet the threshold for significance (for day 3, p=0.076; for day 7, p=0.0582). We did not detect a difference in remaining rows of photoreceptor nuclei.

### 3.7 Optical coherence tomography indicates caspase-11 deficiency may protect against loss of photoreceptors in the sodium iodate model of retinal degeneration

To further evaluate this potential protective effect of caspase-11 deficiency, we again used OCT to measure the ONL thickness *in vivo* (**Figure 3.7**). A trend towards a protective effect on overall ONL thickness was seen in the *Casp11*$^{-/-}$ mouse, although again this effect fell just short of statistical significance (p=0.0508).

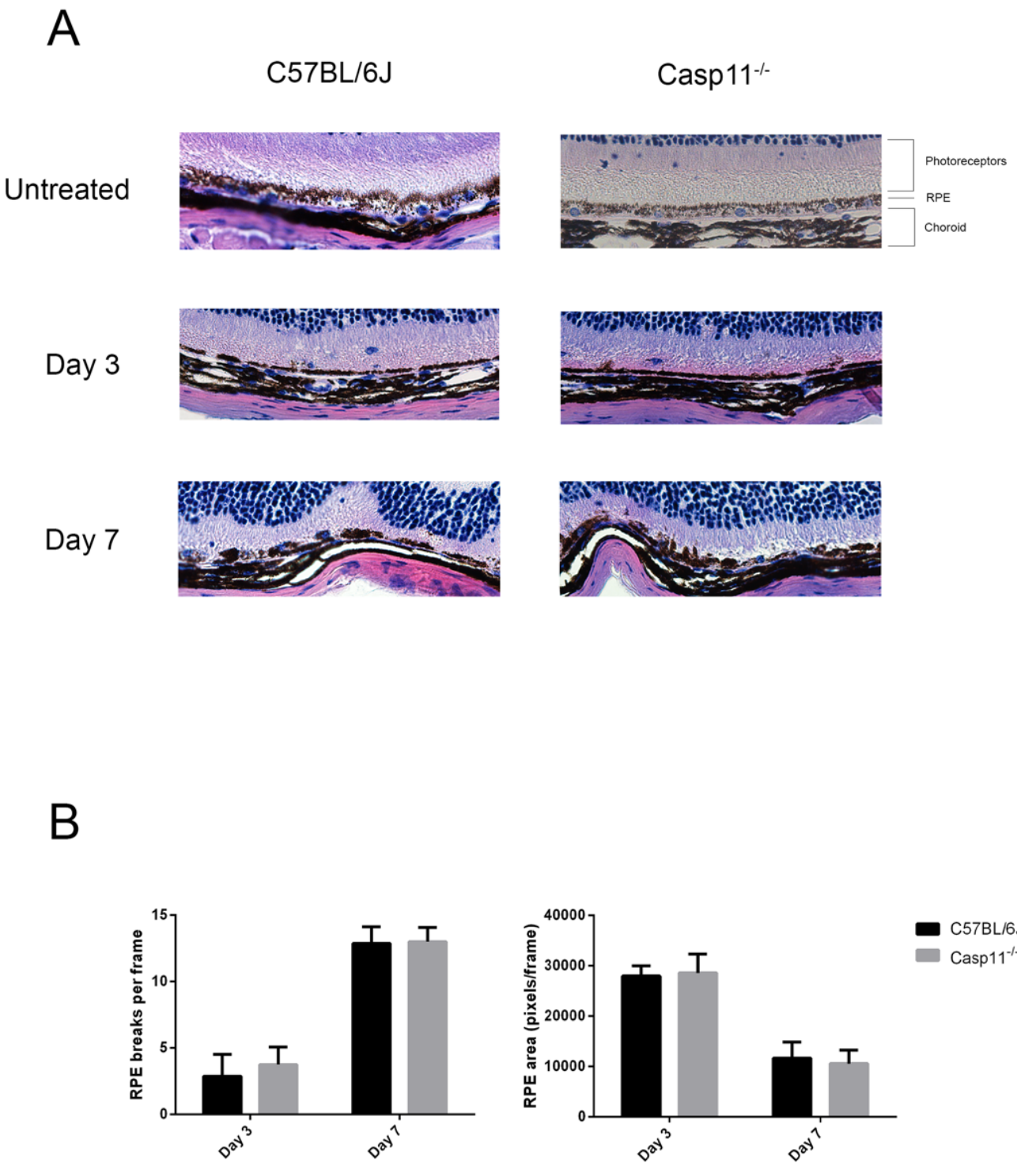


**Figure 3.5 Histology of retinal pigment epithelium (RPE) in wt and *Casp11*$^{-/-}$ mice**

Central and peripheral areas of H&E stained RPE in wt and *Casp11*$^{-/-}$ mice were imaged at 40X magnification and the number of RPE breaks counted and RPE area measured. n=4 for all groups and all mice were female. [A] Representative images at baseline and at days 3 and 7 following administration of sodium iodate. [B] There was no difference seen between the number of RPE breaks or total RPE area at any time point (measurements taken from two central retinal sections per mouse and averaged). Graph displays mean ± SD.

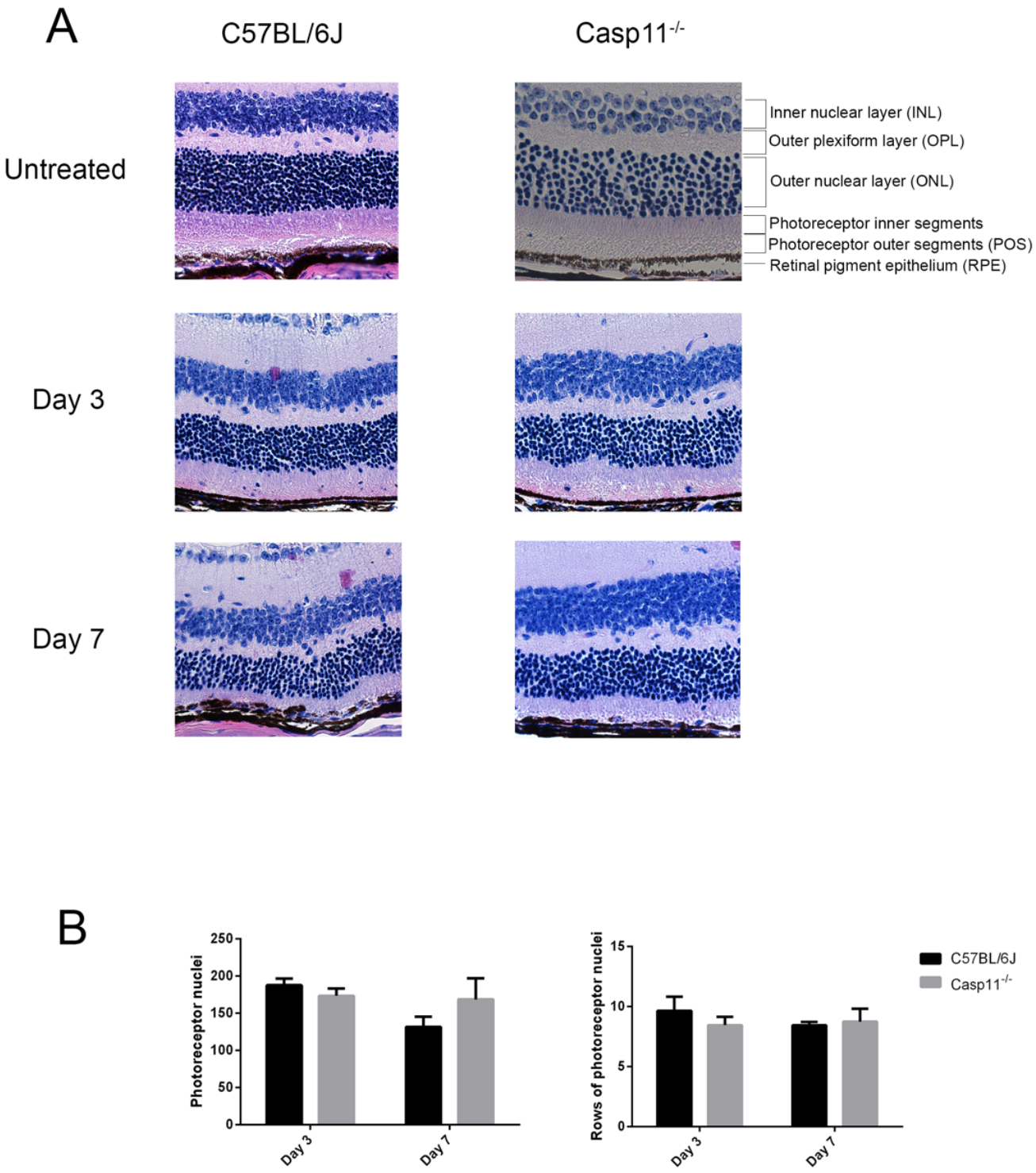


**Figure 3.6 Histology of outer nuclear layer (ONL) in wt and *Casp11*$^{-/-}$ mice**

Central and peripheral areas of H&E stained retinas in wt and *Casp11*$^{-/-}$ mice were imaged at 40X magnification and the photoreceptor nuclei in outer nuclear layer (ONL) were quantified. n=4 for all groups and all mice were female. [A] Representative images at baseline and at days 3 and 7 following administration of sodium iodate. [B] Quantification of photoreceptor nuclei density in outer nuclear layer from two central retinal sections per mouse averaged. Bar diagram shows mean ± SD.

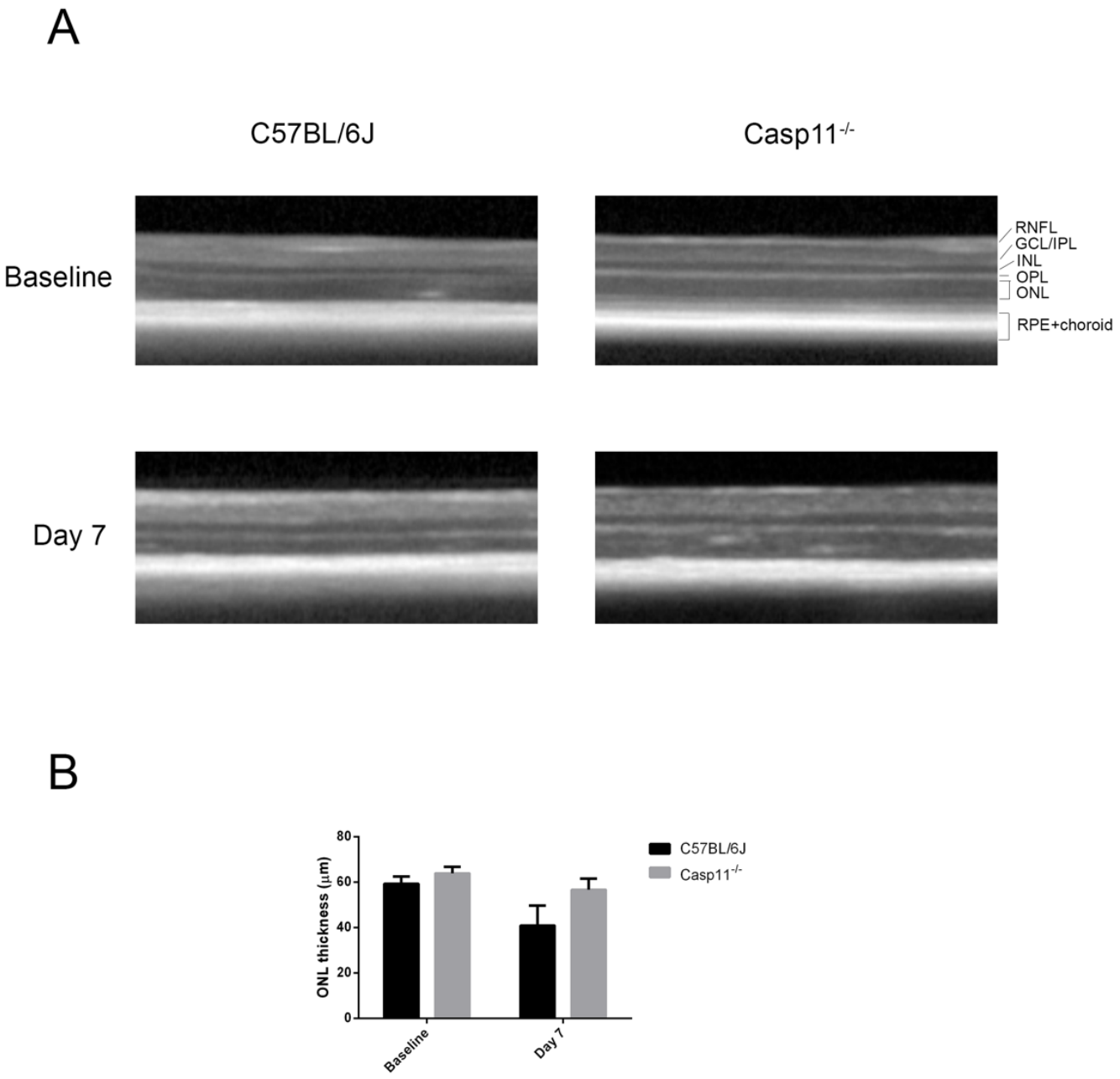


**Figure 3.7 Retinal ONL thickness by OCT in wt and *Casp11*$^{-/-}$ mice**

Cross-sectional *in vivo* OCT images of the posterior pole and nasal and temporal retina in wild-type C57BL/6J mice and *Casp11*$^{-/-}$ mice were taken, with measurement of outer nuclear layer (ONL) thickness. wt n=5, *Casp11*$^{-/-}$ n=4, all female. [A] Representative images at baseline (immediately preceding intervention) and on day 7 following administration of sodium iodate. [B] Bar diagram shows mean ONL thickness as an average of the three regions sampled ± SD. The comparison at day 7 approaches significance (p=0.0508).

### 3.8 Quantification of cell death by TUNEL staining indicates photoreceptors are degenerating at the slower rate in caspase-11 deficient mice compared to wild-type

One possible explanation for the apparent protection of photoreceptors in the caspase-11 deficient mice is that fewer photoreceptors are undergoing cell death in response to sodium iodate. TUNEL staining was performed on retinal sections of *Casp11*$^{-/-}$ and wild-type mice at day 2 and day 7 following sodium iodate (**Figure 3.8**). At day 2, strong TUNEL staining was seen in the ONL of all mice, but by day 7 only occasional TUNEL-positive cells were seen. At day 2, fewer TUNEL positive cells were seen in the retina of *Casp11*$^{-/-}$ mice compared to wild-type ($p=0.036$). At day 7, there was no statistical difference between the groups, although the slightly higher level of TUNEL positivity seen in *Casp11*$^{-/-}$ mice at this timepoint might suggest that photoreceptor cell death was delayed rather than prevented.

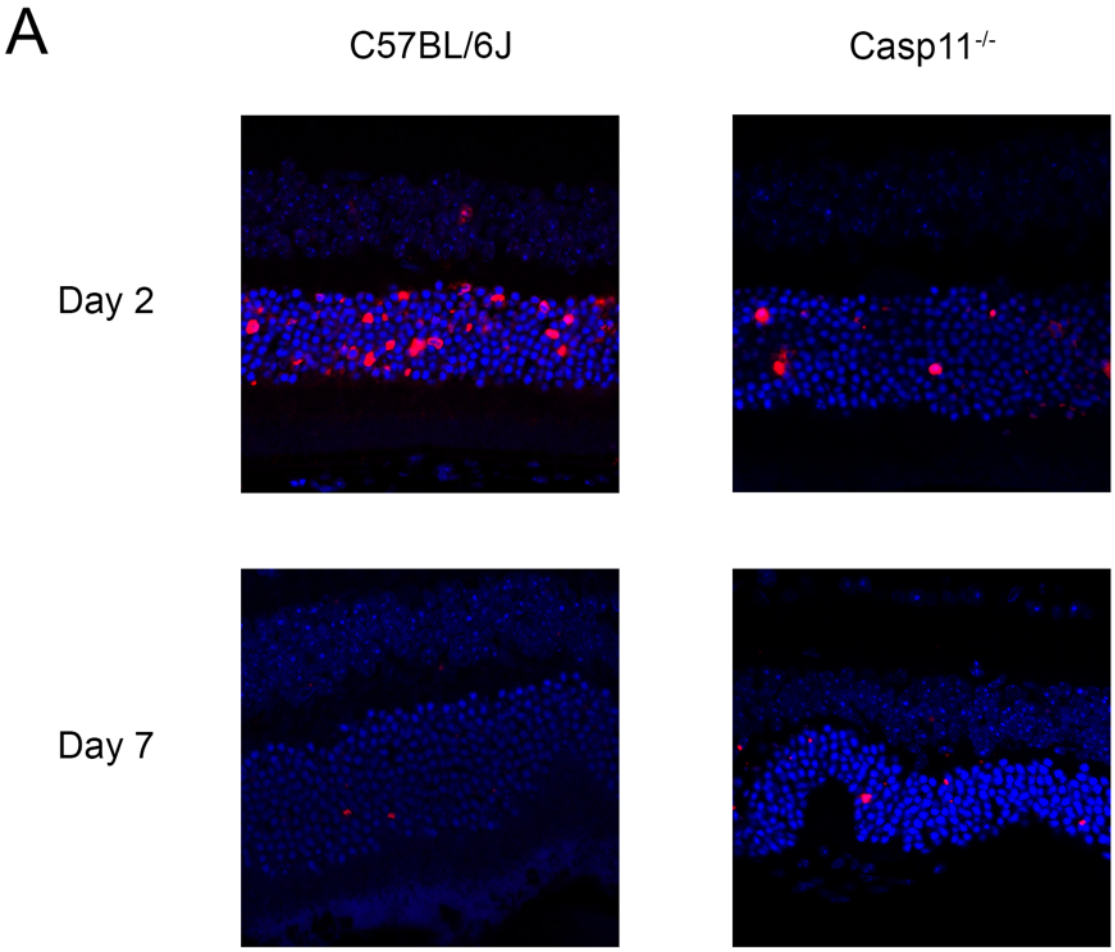


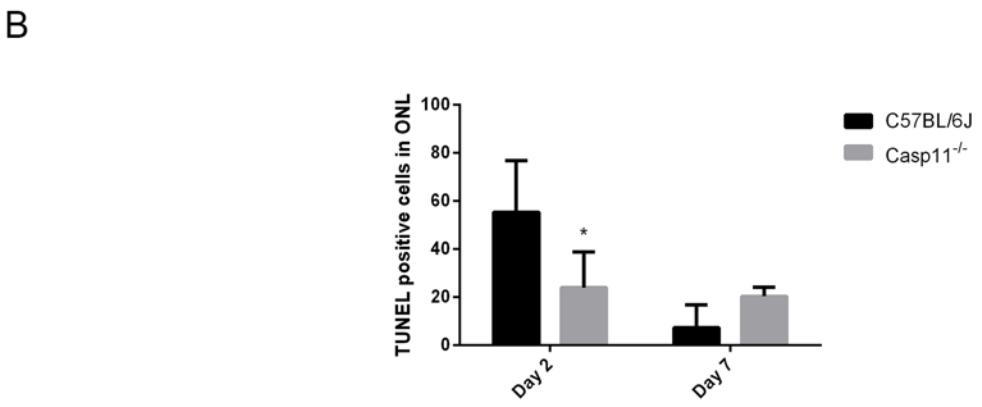


**Figure 3.8 TUNEL staining the ONL in wt and *Casp11*$^{-/-}$ mice**

TUNEL-stained central retinal tissue sections of wild-type and *Casp11*$^{-/-}$ mice were imaged at 40X and number of TUNEL-positive cells in the ONL were measured. Day 2 wt n=4 (two male, two female), *Casp11*$^{-/-}$ n=5 (four male, one female); day 7 wt n=3 (three female), *Casp11*$^{-/-}$ n=4 (three female, one male). [A] Representative images on day 2 and day 7 following administration of sodium iodate. [B] Bar diagram shows number of TUNEL positive cells. Results are an average of eight images across a single central section. Error bars represent mean ± SD. The difference is significant at $p<0.05$ at day 2 but not day 7.

# 4. Discussion

In this study, our aim was to investigate the role of canonical and non-canonical inflammasomes in the sodium iodate mouse as a model of oxidative stress-induced retinal degeneration.

The retinotoxic effects of sodium iodate have been known for decades. It is used in many animal models of retinal degeneration, for example in assessing potential therapies for AMD (Carido *et al.*, 2014). However, much is unknown regarding the mechanisms that underlie cell degeneration in this model. In what manner do photoreceptors die in response to sodium iodate administration? What is the role of inflammation in these processes? How can we reduce or prevent injury?

By using mice deficient for ASC protein, we effectively eliminated any contribution to the resulting retinal damage from the canonical inflammasomes. We showed that despite the inability to produce canonical inflammasomes, there was no difference seen in retinal damage as compared to wild-type mice. This suggests that the major pathogenic mechanisms in the sodium iodate model occur independently of canonical inflammasomes.

In contrast, we showed a trend towards less structural damage in caspase-11-deficient mice when compared with wild-type mice, although our results were not statistically significant. This suggests that caspase-11 and the non-canonical pathways may have a role to play in the retinal damage observed in this model.

The paradigmatic activator of caspase-11 is lipopolysaccharide (LPS), but it is also known that phospholipids can bind to caspase-11 and either antagonise the pro-inflammatory effects of LPS (Chu *et al.*, 2018), or themselves provoke an inflammatory response (Zanoni *et al.*, 2016). We may speculate therefore that part of what is driving caspase-11 in the sodium iodate model is oxidative damage to phospholipids which activates non-canonical inflammasome pathways. Oxidised phospholipids are certainly extensively found in AMD eyes. Alternatively, there may be some as yet unknown trigger to caspase-11 activation.

Our results are somewhat at variance with the finding that using a transfected form of CARD used to prevent caspase-1 activation promotes recovery of the retina from sodium iodate-induced injury (Young *et al.*, 2019). However there are important differences between their methodology and results and ours. A lower dose of sodium iodate (25mg/kg intraperitoneal) was used in this study, which elsewhere has been reported to produce inconsistent results (Chowers *et al.*, 2017). In addition, their main outcome measure in this experiment was electroretinography and not structural changes, and they did not detect any electrophysiological differences at the timepoints we studied, but instead found a recovery effect at four weeks. This may suggest that caspase-1 inhibition has a role in the promotion of longer-term retinal recovery in response to oxidative damage, but does not appear to support its importance in the acute damage phase. Finally, it is entirely possible that inhibiting canonical inflammasomes and inhibiting caspase-1 may produce different results, as it is possible that caspase-1 activation may also occur relatively independently of specific inflammasome sensor proteins (eg NLRP3 or AIM2) (Wooff *et al.*, 2020).

Our findings are also in contrast to another mouse model used in AMD research, the photo-oxidative model. In this model, photoreceptor survival was not improved in mice which lacked caspase-11 (Wooff *et al.*, 2020). There was a small protective effect in *Nlrp3*$^{-/-}$ mice but pharmacological inhibition of NLRP3 with intravitreal MCC950 did not rescue retinal function. In this respect, both their findings and ours suggest that alternative pharmacological avenues other than canonical inflammasome inhibition need to be explored in retinal degeneration. Another mouse with an AMD phenotype, the *Sod1*$^{-/-}$ mouse, has deficiencies in NLRP3 inflammasome function (Deigendesch *et al.*, 2018), but the role of NLRP3 in the retinal findings in this model has not yet been examined.

Caspase inhibition as a therapeutic strategy has been an area of interest, but many of the caspase inhibitors used in research are not suitable for clinical application. For example, while the broad-spectrum caspase inhibitor Z-VAD-FMK reduces hyperglycemia-induced apoptosis in rat retinal Muller cells (Mohr *et al.*, 2002), this inhibitor is not suitable for human use due to high levels of toxicity (Van Noorden, 2001). However newer small-molecule caspase inhibitors have been developed and some have entered clinical testing.

Emricasan is an irreversible pan-caspase inhibitor which can be administered orally and showed some promise in animal models of liver disease (Eguchi *et al.*, 2018). However subsequent randomised controlled trials demonstrated no improvement in non-alcoholic steatohepatitis (Frenette *et al.*, 2021; Garcia-Tsao *et al.*, 2020; Harrison *et al.*, 2020). Nevertheless, these studies were useful in that they appeared to confirm that emricasan is safe and well-tolerated for human use.

Two other oral caspase inhibitors nivocasan (caspases-1, -8, and -9) and pralnacasan (caspase-1) were suspended from clinical investigation due to safety concerns (Kudelova *et al.*, 2015; MacKenzie *et al.*, 2010). A further caspase-1 inhibitor belnacasan was under investigation in two clinical trials (ClinicalTrials.gov NCT01501383 and NCT00205465) which concluded without publication of results. Interestingly, a randomised controlled trial of belnacasan was recently performed in patients with COVID-19, although it is yet to report its findings (ClinicalTrials.gov NCT05164120). None of these caspase inhibitors have been used in a retinal context, although belnacasan has been used on trabecular meshwork cells (L. Li *et al.*, 2021).

With regard to pharmacological inhibition of caspase-11, one substance which has been studied is the herbal medicine-derivative wedelolactone (Kobori *et al.*, 2004). This substance has multiple mechanisms of action and appears to have a broad anti-inflammatory and anti-oxidant effects (for summary of reported actions, see recent review at Ha *et al*., 2023). One effect of interest is downregulating caspase-11 activation (Kobori *et al.*, 2004).

Of relevance to our current work, wedelolactone delivered intravitreally was used to protect against chemically-induced retinal degeneration with N-methyl-N-nitrosourea (NMU) (Harkin *et al.*, 2022). NMU is an alkylating agent which damages DNA, and although the exact process by which NMU causes retinal degeneration is not fully understood, as in sodium iodate, oxidative stress is believed to play a major role (Tsuruma *et al.*, 2012). Harkin *et al*. found that NMU upregulated AIM2, caspase-11 and caspase-1 in the mouse retina but had no significant effect on NLRP3 or Il-1$\beta$. The protection (both histological

and electroretinographical) afforded by wedelolactone appeared to be mediated at least partially by wedelolactone's inhibition of the Aim2/caspase-11/IL-18 pathway.

This suggests that in an alternative model of oxidative stress-induced retinal degeneration to our own, caspase-11 is an important pathological factor. The authors hypothesised that cytosolic release of DNA by NMU upregulates the AIM2 inflammasome, whose primary activator is DNA. There is some support for the role of AIM2 in the pathogenesis of AMD, as induced pluripotent stem-cell-derived RPE cells (iPSC-RPE) from a patient with AMD had higher levels of AIM2 gene expression in response to stressors, while there was no difference in NLRP3 (Hytti *et al.*, 2021). However, in contrast to this, our use of ASC knock-out mice suggests that the involvement of caspase-11 in the sodium iodate model occurs independently of AIM2, as AIM2 has been shown to require functional ASC for its processing of multiple caspases (Sagulenko *et al.*, 2013).

The effect wedelolactone has on the non-canonical inflammasome pathways has also been explored in other eye tissues: in Pseudomonas aeruginosa corneal infections, wedelolactone was found to reduce injury via downregulation of caspase-4/5/11 non-canonical inflammasomes (S. Xu *et al.*, 2021). However, given the multitude of pathways that wedelolactone affects, a primary role for caspase-11 inhibition has not been clearly established: in other models of non-ocular disease, wedelolactone has been shown to have effects on the NLRP3 inflammasome (Bhattacharyya & Law, 2022; Pan *et al.*, 2020). In addition, rather puzzlingly it has also been reported that wedelolactone administration actually increases ROS generation and pyroptosis via caspase-1 in retinoblastoma cells, with no effect on caspase-11. This is quite different to the anti-pyroptotic effects reported

elsewhere, for example in acute pancreatitis (Fan *et al.*, 2021) and acute liver injury (Lu *et al.*, 2016), suggesting context-specific differential effects.

The dose of sodium iodate we used was 70mg/kg by intraperitoneal injection. Multiple dosing regimens and methods of administration are described. A classic study used an intraperitoneal dose of 100mg/kg (Kiuchi *et al.*, 2002). They reported very early damage to the RPE (seen at 6 hours) followed by outer segment disruption and photoreceptor loss which was maximal at day 3 and was completed by day 7. Chowers *et al*. (2017) more recently investigated a range of intraperitoneal doses (25, 50, and 100mg/kg) and found there was substantial systemic toxicity and mortality associated with the 100mg/kg dose. At the lower doses these systemic effects were not seen, but the 25mg/kg dose was found to produce very inconsistent results. At our dosing of 70mg/kg, we saw consistent retinal damage without systemic toxicity.

There are also several potential methods of delivery of sodium iodate to induce retinal degeneration, the two most commonly used being intraperitoneal or intravenously by tail vein injection. Other more rarely used delivery methods include retro-orbital (Machalińska *et al.*, 2010; J. Wang *et al.*, 2014), intravitreal (Ahn *et al.*, 2019; Cho *et al.*, 2016), and subretinal injection (Bhutto *et al.*, 2018).

Tail vein injections can be technically difficult and leaks are a potential source of variability. The degree of injection failure in fact is probably under-recognised (Groman & Reinhardt, 2004) although it can also be argued that when performed correctly they ensure a repeatable concentration of sodium iodate in the blood. Retro-orbital, intravitreal, and subretinal injections have the theoretical advantage of delivering sodium

iodate close to the target retinal tissue, but these procedures can be technically demanding, require anaesthesia, and risk direct injury to the eye. For example, inducing consistent, diffuse retinal degeneration with intravitreal sodium iodate seems to require the eye to be vitrectomised beforehand (Ahn *et al.*, 2019), which carries a significant morbidity (40% in that study developed media opacities). These procedures tend to be performed in larger animals than mice.

There also appears to be a difference in the primary site of injury depending on method of administration: intravitreal delivery appears to damage the photoreceptors and associated retinal architecture while the RPE cells remain normal (Ahn *et al.*, 2019); while subretinal delivery appears to induce localised, well-circumscribed damage to retina and RPE only in the area of the subretinal bleb (Monés *et al.*, 2016). Results are therefore not comparable to the studies done with systemic sodium iodate administration. We chose intraperitoneal delivery as it is easily performed and appears to produce consistent results.

In our first experiment in *Pycard*$^{-/-}$ mice, we initially used a mix of male and female animals. Yang *et al*. (2021) reported that very few studies in this area to date publish the sex mix of the animals used. Initial morphological studies had suggested there was no sex difference in the response to sodium iodate (Kiuchi *et al.*, 2002). However, over the course of this experiment and others, we had noted that the sex of the mouse may have an effect on the degree of retinal damage, with males developing a worse phenotype. In subsequent experiments we used only female animals, as we wanted to eliminate sex difference as a potential confounding factor. While little has been published on sex differences in the sodium iodate mouse, recently in a collagen-induced arthritis model of

inflammatory arthritis, it was reported that sodium iodate (50mg/kg intraperitoneally) caused a greater decrease in retinal thickness at day 10 in male mice compared with females (Schnabolk *et al.*, 2020).

However, another group has published the opposite finding: Yang *et al*. (2021) using low-dose sodium iodate (10-11mg/kg) found that the RPE of female mice was more susceptible to damage at seven days than that of male mice. They speculate that the high dose of sodium iodate used in many experiments could conceivably have masked sex-based differences. Some significant caveats apply to this study however. Firstly, this study was on RPE flatmounts and so did not examine the effect on the retina. In addition, the dose of sodium iodate used was much lower than most other studies, and many others have reported that doses in this range produces minimal or inconsistent retinal damage. For example, a dose of 10mg/kg intravenously was not found by another group to cause consistent retinal damage as assessed by electroretinogram (ERG), and they report that at least 15mg/kg was necessary to reliably induce RPE damage (Zhang *et al.*, 2021). Another group found there was no change in retinal thickness on OCT out to 62 days in their 10-20mg/kg group, although temporary changes in ERG were noted (Koster *et al.*, 2022).

Finally, in lower dose sodium iodate, it may be the case that a day 7 timepoint is insufficient to demonstrate its damaging effect adequately. Koster *et al*. (2022) reported that mice exposed to doses up to 30mg/kg intravenously showed no retinal degeneration by OCT at 7 days, and RPE thinning and disruption of retinal architecture only began to appear at 13 days in the 30mg/kg group. In contrast, with higher doses (40-70mg/kg) similar to ours, retinal thinning on OCT was visible within a week.

When we performed the initial experiment in *Pycard*$^{-/-}$ mice, we selected days 1, 2, and 7 as our timepoints for analysis. In our experience, the majority of damage to the ONL was complete by day 7. This accords with the findings in Carido *et al*., (2014) that ONL thickness following sodium iodate administration remained essentially constant from day 7 to day 28, with the main reduction occurring between day 3 and day 7. This correlated with the ERG findings, with rod responses abolished by day 3 and the remainder of responses declining to nothing by day 14. The earlier timepoints in our initial *Pycard*$^{-/-}$ experiment were chosen in the hope of demonstrating any early effects of sodium iodate. However, it became apparent that there were not sufficient changes on a histological level at day 1 to extrapolate a meaningful differences between mice. For our subsequent *Casp11*$^{-/-}$ experiment, we chose day 3 and 7 as our timepoints.

Our study has some limitations. The numbers of mice in each group were small (n=4-6). With respect to the *Pycard*$^{-/-}$ mice, we cannot exclude the possibility the *Pycard*$^{-/-}$ mice had some small protective effect beneath the threshold of our ability to detect in this experiment. Some of the measurements used require a degree of subjective judgement: the measurement of rows of photoreceptor nuclei, while used in retinal research for several decades (Cayouette & Gravel, 1997), can be difficult to perform, particularly where the architecture of the retina has become very disturbed and the distinct layers are more difficult to appreciate. Nevertheless, in the more objective measure of number of photoreceptor nuclei per area of ONL segment, there was a difference between *Casp11*$^{-/-}$ and wild-type mice (although not reaching the level of statistical significance).

As a model of AMD, the sodium iodate mouse has some shortcomings. We know that oxidative stress plays an important part in the development of AMD, but there will be

obvious differences between this chronic form of daily oxidative stress and the acute and massive oxidative stress imposed by sodium iodate administration.

Moreover, while mice are easier to work with than larger animals, their use presents problems when comparing to higher animals or to humans (Kostic & Arsenijevic, 2016). Rodents lack a central concentration of retinal photoreceptors which is present in, for example, pigs. However, while the retina of the pig probably bears the closest resemblance to the human retina aside from other primates, the pig's area centralis is still quite different to the human macula (Kostic & Arsenijevic, 2016). In addition, researchers have so far been unable to investigate sodium iodate retinal toxicity in a porcine model due to the fact that sodium iodate does not induce retinal degeneration in pigs at a sublethal dose (Noel *et al.*, 2012).

We used mice of the widely available C57BL/6 strain. Zhang *et al*. (2021) found that there were differences on electrophysiologic and morphological responses to low-dose sodium iodate delivered intravenously according to the strain of mouse used, so caution must be exercised in comparing to studies in other mice.

While we investigated morphological measures of photoreceptor loss, assessing retinal function in animals generally requires electrophysiological measures, usually electroretinogram (ERG). While we did not perform ERG in our animals, it is important to note that in retinal degeneration models structural measures generally correlate with functional measures (Adachi *et al.*, 2016; Kadkhodaeian *et al.*, 2016). Additionally, in the acute severe injury induced by sodium iodate, the early extreme effect on the ERG can preclude meaningful comparison; for example, one study found that by day 3 following

sodium iodate administration, b-wave measurements were completely abolished and undetectable (Machalińska *et al.*, 2010).

In summary we investigated the role of canonical and non-canonical inflammasomes in the sodium iodate mouse. We were unable to demonstrate any protective effect from blocking canonical inflammasome activation in this model, while there was a trend towards protection in non-canonical inflammasome inhibition. Further work in this area is necessary.

## References


Adachi, K., Takahashi, S., Yamauchi, K., Mounai, N., Tanabu, R., & Nakazawa, M. (2016). Optical Coherence Tomography of Retinal Degeneration in Royal College of Surgeons Rats and Its Correlation with Morphology and Electroretinography. *PLOS ONE*, *11*(9), e0162835. https://doi.org/10.1371/journal.pone.0162835

Afonina, I. S., Zhong, Z., Karin, M., & Beyaert, R. (2017). Limiting inflammation—the negative regulation of NF-κB and the NLRP3 inflammasome. *Nature Immunology*, *18*(8), 861–869. https://doi.org/10.1038/ni.3772

Ahn, S. M., Ahn, J., Cha, S., Yun, C., Park, T. K., Kim, Y.-J., Goo, Y. S., & Kim, S.-W. (2019). The effects of intravitreal sodium iodate injection on retinal degeneration following vitrectomy in rabbits. *Scientific Reports*, *9*(1), 15696. https://doi.org/10.1038/s41598-019-52172-y

Akuffo, K. O., Nolan, J., Stack, J., Moran, R., Feeney, J., Kenny, R. A., Peto, T., Dooley, C., O'Halloran, A. M., Cronin, H., & Beatty, S. (2015). Prevalence of age-related macular degeneration in the Republic of Ireland. *British Journal of Ophthalmology*, *99*(8), 1037–1044. https://doi.org/10.1136/bjophthalmol-2014-305768

Ambati, J., Anand, A., Fernandez, S., Sakurai, E., Lynn, B. C., Kuziel, W. A., Rollins, B. J., & Ambati, B. K. (2003). An animal model of age-related macular degeneration in senescent Ccl-2- or Ccr-2-deficient mice. *Nature Medicine*, *9*(11), 1390–1397. https://doi.org/10.1038/nm950

Ambati, J., Atkinson, J. P., & Gelfand, B. D. (2013). Immunology of age-related macular degeneration. *Nature Reviews Immunology*, *13*(6), 438–451.

https://doi.org/10.1038/nri3459

Anderson, O. A., Finkelstein, A., & Shima, D. T. (2013). A2E Induces IL-1ß Production in Retinal Pigment Epithelial Cells via the NLRP3 Inflammasome. *PLoS ONE*, *8*(6), e67263. https://doi.org/10.1371/journal.pone.0067263

Aredo, B., Li, T., Chen, X., Zhang, K., Wang, C. X.-Z., Gou, D., Zhao, B., He, Y., & Ufret-Vincenty, R. L. (2015). A Chimeric Cfh Transgene Leads to Increased Retinal Oxidative Stress, Inflammation, and Accumulation of Activated Subretinal Microglia in Mice. *Investigative Opthalmology & Visual Science*, *56*(6), 3427. https://doi.org/10.1167/iovs.14-16089

Baich, A., & Ziegler, M. (1992). The effect of sodium iodate and melanin on the formation of glyoxylate. *Pigment Cell Research*, *5*(6), 394–395. https://doi.org/10.1111/j.1600-0749.1992.tb00568.x

Balmer, J., Zulliger, R., Roberti, S., & Enzmann, V. (2015). Retinal Cell Death Caused by Sodium Iodate Involves Multiple Caspase-Dependent and Caspase-Independent Cell-Death Pathways. *International Journal of Molecular Sciences*, *16*(12), 15086–15103. https://doi.org/10.3390/ijms160715086

Berghe, T. Vanden, Vanlangenakker, N., Parthoens, E., Deckers, W., Devos, M., Festjens, N., Guerin, C. J., Brunk, U. T., Declercq, W., & Vandenabeele, P. (2010). Necroptosis, necrosis and secondary necrosis converge on similar cellular disintegration features. *Cell Death & Differentiation*, *17*(6), 922–930. https://doi.org/10.1038/cdd.2009.184

Bergsbaken, T., Fink, S. L., & Cookson, B. T. (2009). Pyroptosis: host cell death and inflammation. *Nature Reviews Microbiology*, *7*(2), 99–109.

https://doi.org/10.1038/nrmicro2070

Bhattacharyya, S., & Law, S. (2022). Environmental pollutant N-N'ethylnitrosourea-induced leukemic NLRP3 inflammasome activation and its amelioration by Eclipta prostrata and its active compound wedelolactone. *Environmental Toxicology*, *37*(2), 322–334. https://doi.org/10.1002/tox.23400

Bhutto, I. A., Ogura, S., Baldeosingh, R., McLeod, D. S., Lutty, G. A., & Edwards, M. M. (2018). An Acute Injury Model for the Phenotypic Characteristics of Geographic Atrophy. *Investigative Opthalmology & Visual Science*, *59*(4), AMD143. https://doi.org/10.1167/iovs.18-24245

Campochiaro, P. A., & Mir, T. A. (2018). The mechanism of cone cell death in Retinitis Pigmentosa. *Progress in Retinal and Eye Research*, *62*, 24–37. https://doi.org/10.1016/j.preteyeres.2017.08.004

Cao, S., Ko, A., Partanen, M., Pakzad-Vaezi, K., Merkur, A. B., Albiani, D. A., Kirker, A. W., Wang, A., Cui, J. Z., Forooghian, F., & Matsubara, J. A. (2013). Relationship between systemic cytokines and complement factor H Y402H polymorphism in patients with dry age-related macular degeneration. *American Journal of Ophthalmology*, *156*(6), 1176–1183. https://doi.org/10.1016/j.ajo.2013.08.003

Carido, M., Zhu, Y., Postel, K., Benkner, B., Cimalla, P., Karl, M. O., Kurth, T., Paquet-Durand, F., Koch, E., Münch, T. A., Tanaka, E. M., & Ader, M. (2014). Characterization of a Mouse Model With Complete RPE Loss and Its Use for RPE Cell Transplantation. *Investigative Opthalmology & Visual Science*, *55*(8), 5431. https://doi.org/10.1167/iovs.14-14325

Carty, M., Kearney, J., Shanahan, K. A., Hams, E., Sugisawa, R., Connolly, D., Doran, C. G.,

Muñoz-Wolf, N., Gürtler, C., Fitzgerald, K. A., Lavelle, E. C., Fallon, P. G., & Bowie, A. G. (2019). Cell Survival and Cytokine Release after Inflammasome Activation Is Regulated by the Toll-IL-1R Protein SARM. *Immunity*, *50*(6), 1412-1424.e6. https://doi.org/10.1016/j.immuni.2019.04.005

Cayouette, M., & Gravel, C. (1997). Adenovirus-Mediated Gene Transfer of Ciliary Neurotrophic Factor Can Prevent Photoreceptor Degeneration in the Retinal Degeneration ( rd ) Mouse. *Human Gene Therapy*, *8*(4), 423–430. https://doi.org/10.1089/hum.1997.8.4-423

Chen, X., He, W., Hu, L., Li, J., Fang, Y., Wang, X., Xu, X., Wang, Z., Huang, K., & Han, J. (2016). Pyroptosis is driven by non-selective gasdermin-D pore and its morphology is different from MLKL channel-mediated necroptosis. *Cell Research*, *26*(9), 1007–1020. https://doi.org/10.1038/cr.2016.100

Cho, B.-J., Seo, J.-M., Yu, H. G., & Chung, H. (2016). Monocular retinal degeneration induced by intravitreal injection of sodium iodate in rabbit eyes. *Japanese Journal of Ophthalmology*, *60*(3), 226–237. https://doi.org/10.1007/s10384-016-0429-1

Chowers, G., Cohen, M., Marks-Ohana, D., Stika, S., Eijzenberg, A., Banin, E., & Obolensky, A. (2017). Course of Sodium Iodate–Induced Retinal Degeneration in Albino and Pigmented Mice. *Investigative Opthalmology & Visual Science*, *58*(4), 2239. https://doi.org/10.1167/iovs.16-21255

Christofferson, D. E., & Yuan, J. (2010). Necroptosis as an alternative form of programmed cell death. *Current Opinion in Cell Biology*, *22*(2), 263–268. https://doi.org/10.1016/j.ceb.2009.12.003

Chu, L. H., Indramohan, M., Ratsimandresey, R. A., Gangopadhyay, A., Morris, E. P.,

Monack, D. M., Dorfleutner, A., & Stehlik, C. (2018). The oxidized phospholipid oxPAPC protects from septic shock by targeting the non-canonical inflammasome in macrophages. *Nature Communications*, *9*(1), 996. https://doi.org/10.1038/s41467-018-03409-3

Coffey, P. J., Gias, C., McDermott, C. J., Lundh, P., Pickering, M. C., Sethi, C., Bird, A., Fitzke, F. W., Maass, A., Chen, L. L., Holder, G. E., Luthert, P. J., Salt, T. E., Moss, S. E., & Greenwood, J. (2007). Complement factor H deficiency in aged mice causes retinal abnormalities and visual dysfunction. *Proceedings of the National Academy of Sciences*, *104*(42), 16651–16656. https://doi.org/10.1073/pnas.0705079104

Cooke, M. S., Evans, M. D., Dizdaroglu, M., & Lunec, J. (2003). Oxidative DNA damage: mechanisms, mutation, and disease. *The FASEB Journal*, *17*(10), 1195–1214. https://doi.org/10.1096/fj.02-0752rev

Corazza, P., D'Alterio, F. M., Kabbani, J., Alam, M. M. R., Mercuri, S., Orlans, H. O., & Younis, S. (2021). Long-term outcomes of intravitreal anti-VEGF therapies in patients affected by neovascular age-related macular degeneration: a real-life study. *BMC Ophthalmology*, *21*(1), 300. https://doi.org/10.1186/s12886-021-02055-6

Cox, J. T., Eliott, D., & Sobrin, L. (2021). Inflammatory Complications of Intravitreal Anti-VEGF Injections. *Journal of Clinical Medicine*, *10*(5), 981. https://doi.org/10.3390/jcm10050981

Crane, I. J., & Liversidge, J. (2008). Mechanisms of leukocyte migration across the blood–retina barrier. *Seminars in Immunopathology*, *30*(2), 165–177. https://doi.org/10.1007/s00281-008-0106-7

Davis, B. K., Roberts, R. A., Huang, M. T., Willingham, S. B., Conti, B. J., Brickey, W. J., Barker, B. R., Kwan, M., Taxman, D. J., Accavitti-Loper, M.-A., Duncan, J. A., & Ting, J. P.-Y. (2011). Cutting Edge: NLRC5-Dependent Activation of the Inflammasome. *The Journal of Immunology*, *186*(3), 1333–1337. https://doi.org/10.4049/jimmunol.1003111

de Carvalho, R. V. H., Andrade, W. A., Lima-Junior, D. S., Dilucca, M., de Oliveira, C. V., Wang, K., Nogueira, P. M., Rugani, J. N., Soares, R. P., Beverley, S. M., Shao, F., & Zamboni, D. S. (2019). Leishmania Lipophosphoglycan Triggers Caspase-11 and the Non-canonical Activation of the NLRP3 Inflammasome. *Cell Reports*, *26*(2), 429-437.e5. https://doi.org/10.1016/j.celrep.2018.12.047

Deigendesch, N., Zychlinsky, A., & Meissner, F. (2018). Copper Regulates the Canonical NLRP3 Inflammasome. *The Journal of Immunology*, ji1700712. https://doi.org/10.4049/jimmunol.1700712

Delori, F. C., Goger, D. G., Hammond, B. R., Snodderly, D. M., & Burns, S. A. (2001). Macular pigment density measured by autofluorescence spectrometry: comparison with reflectometry and heterochromatic flicker photometry. *Journal of the Optical Society of America A*, *18*(6), 1212. https://doi.org/10.1364/JOSAA.18.001212

Dentchev, T., Milam, A. H., Lee, V. M.-Y., Trojanowski, J. Q., & Dunaief, J. L. (2003). Amyloid-beta is found in drusen from some age-related macular degeneration retinas, but not in drusen from normal retinas. *Molecular Vision*, *9*, 184–190. http://www.ncbi.nlm.nih.gov/pubmed/12764254

Diaz-Araya, C. M., Provis, J. M., Penfold, P. L., & Billson, F. A. (1995). Development of microglial topography in human retina. *The Journal of Comparative Neurology*,

*363*(1), 53–68. https://doi.org/10.1002/cne.903630106

Dinarello, C. A. (2009). Immunological and Inflammatory Functions of the Interleukin-1 Family. *Annual Review of Immunology*, *27*(1), 519–550. https://doi.org/10.1146/annurev.immunol.021908.132612

Doyle, S. L., Campbell, M., Ozaki, E., Salomon, R. G., Mori, A., Kenna, P. F., Farrar, G. J., Kiang, A.-S., Humphries, M. M., Lavelle, E. C., O'Neill, L. A. J., Hollyfield, J. G., & Humphries, P. (2012). NLRP3 has a protective role in age-related macular degeneration through the induction of IL-18 by drusen components. *Nature Medicine*, *18*(5), 791–798. https://doi.org/10.1038/nm.2717

Eguchi, A., Koyama, Y., Wree, A., Johnson, C. D., Nakamura, R., Povero, D., Kneiber, D., Tameda, M., Contreras, P., Spada, A., & Feldstein, A. E. (2018). Emricasan, a pan-caspase inhibitor, improves survival and portal hypertension in a murine model of common bile-duct ligation. *Journal of Molecular Medicine*, *96*(6), 575–583. https://doi.org/10.1007/s00109-018-1642-9

Enzbrenner, A., Zulliger, R., Biber, J., Pousa, A. M. Q., Schäfer, N., Stucki, C., Giroud, N., Berrera, M., Kortvely, E., Schmucki, R., Badi, L., Grosche, A., Pauly, D., & Enzmann, V. (2021). Sodium Iodate-Induced Degeneration Results in Local Complement Changes and Inflammatory Processes in Murine Retina. *International Journal of Molecular Sciences*, *22*(17), 9218. https://doi.org/10.3390/ijms22179218

Fan, R., Sui, J., Dong, X., Jing, B., & Gao, Z. (2021). Wedelolactone alleviates acute pancreatitis and associated lung injury via GPX4 mediated suppression of pyroptosis and ferroptosis. *Free Radical Biology and Medicine*, *173*, 29–40.

Fields, M. A., Del Priore, L. V., Adelman, R. A., & Rizzolo, L. J. (2020). Interactions of the

choroid, Bruch's membrane, retinal pigment epithelium, and neurosensory retina collaborate to form the outer blood-retinal-barrier. *Progress in Retinal and Eye Research*, *76*, 100803. https://doi.org/10.1016/j.preteyeres.2019.100803

Forrester, J. V., McMenamin, P. G., & Dando, S. J. (2018). CNS infection and immune privilege. *Nature Reviews Neuroscience*, *19*(11), 655–671. https://doi.org/10.1038/s41583-018-0070-8

Franco, L. M., Zulliger, R., Wolf-Schnurrbusch, U. E. K., Katagiri, Y., Kaplan, H. J., Wolf, S., & Enzmann, V. (2009). Decreased Visual Function after Patchy Loss of Retinal Pigment Epithelium Induced by Low-Dose Sodium Iodate. *Investigative Opthalmology & Visual Science*, *50*(8), 4004. https://doi.org/10.1167/iovs.08-2898

Frenette, C., Kayali, Z., Mena, E., Mantry, P. S., Lucas, K. J., Neff, G., Rodriguez, M., Thuluvath, P. J., Weinberg, E., Bhandari, B. R., Robinson, J., Wedick, N., Chan, J. L., Hagerty, D. T., Kowdley, K. V., Corey, K., Bernstein, D., Noureddin, M., Kemmer, N., … Patel, B. (2021). Emricasan to prevent new decompensation in patients with NASH-related decompensated cirrhosis. *Journal of Hepatology*, *74*(2), 274–282. https://doi.org/10.1016/j.jhep.2020.09.029

Gabrielli, E., Pericolini, E., Luciano, E., Sabbatini, S., Roselletti, E., Perito, S., Kasper, L., Hube, B., & Vecchiarelli, A. (2015). Induction of Caspase-11 by Aspartyl Proteinases of Candida albicans and Implication in Promoting Inflammatory Response. *Infection and Immunity*, *83*(5), 1940–1948. https://doi.org/10.1128/IAI.02895-14

Garcia-Tsao, G., Bosch, J., Kayali, Z., Harrison, S. A., Abdelmalek, M. F., Lawitz, E., Satapathy, S. K., Ghabril, M., Shiffman, M. L., Younes, Z. H., Thuluvath, P. J., Berzigotti, A., Albillos, A., Robinson, J. M., Hagerty, D. T., Chan, J. L., Sanyal, A. J.,

Abdelmalek, M., Bhamidimarri, K., … Muellhaupt, B. (2020). Randomized placebo-controlled trial of emricasan for non-alcoholic steatohepatitis-related cirrhosis with severe portal hypertension. *Journal of Hepatology*, *72*(5), 885–895. https://doi.org/10.1016/j.jhep.2019.12.010

Gibbons, L., Ozaki, E., Greene, C., Trappe, A., Carty, M., Coppinger, J. A., Bowie, A. G., Campbell, M., & Doyle, S. L. (2022). SARM1 Promotes Photoreceptor Degeneration in an Oxidative Stress Model of Retinal Degeneration. *Frontiers in Neuroscience*, *16*. https://doi.org/10.3389/fnins.2022.852114

Groman, E. V, & Reinhardt, C. P. (2004). Method to quantify tail vein injection technique in small animals. *Contemporary Topics in Laboratory Animal Science*, *43*(1), 35–38. http://www.ncbi.nlm.nih.gov/pubmed/14984288

Guillonneau, X., Eandi, C. M., Paques, M., Sahel, J.-A., Sapieha, P., & Sennlaub, F. (2017). On phagocytes and macular degeneration. *Progress in Retinal and Eye Research*, *61*, 98–128. https://doi.org/10.1016/j.preteyeres.2017.06.002

Guo, H., Callaway, J. B., & Ting, J. P.-Y. (2015). Inflammasomes: mechanism of action, role in disease, and therapeutics. *Nature Medicine*, *21*(7), 677–687. https://doi.org/10.1038/nm.3893

Gupta, N., Brown, K. E., & Milam, A. H. (2003). Activated microglia in human retinitis pigmentosa, late-onset retinal degeneration, and age-related macular degeneration. *Experimental Eye Research*, *76*(4), 463–471. https://doi.org/10.1016/S0014-4835(02)00332-9

Ha, N. M., Hop, N. Q., & Son, N. T. (2023). Wedelolactone: A molecule of interests. *Fitoterapia*, *164*, 105355. https://doi.org/10.1016/j.fitote.2022.105355

Hageman, G. S., Luthert, P. J., Victor Chong, N. H., Johnson, L. V., Anderson, D. H., & Mullins, R. F. (2001). An integrated hypothesis that considers drusen as biomarkers of immune-mediated processes at the RPE-Bruch's membrane interface in aging and age-related macular degeneration. *Progress in Retinal and Eye Research*, *20*(6), 705–732. https://doi.org/10.1016/S1350-9462(01)00010-6

Hahn, P., Qian, Y., Dentchev, T., Chen, L., Beard, J., Harris, Z. L., & Dunaief, J. L. (2004). Disruption of ceruloplasmin and hephaestin in mice causes retinal iron overload and retinal degeneration with features of age-related macular degeneration. *Proceedings of the National Academy of Sciences*, *101*(38), 13850–13855. https://doi.org/10.1073/pnas.0405146101

Handa, J. T., Verzijl, N., Matsunaga, H., Aotaki-Keen, A., Lutty, G. A., te Koppele, J. M., Miyata, T., & Hjelmeland, L. M. (1999). Increase in the advanced glycation end product pentosidine in Bruch's membrane with age. *Investigative Ophthalmology & Visual Science*, *40*(3), 775–779. http://www.ncbi.nlm.nih.gov/pubmed/10067983

Hanus, J., Anderson, C., Sarraf, D., Ma, J., & Wang, S. (2016). Retinal pigment epithelial cell necroptosis in response to sodium iodate. *Cell Death Discovery*, *2*(1), 16054. https://doi.org/10.1038/cddiscovery.2016.54

Hanus, J., Zhang, H., Wang, Z., Liu, Q., Zhou, Q., & Wang, S. (2013). Induction of necrotic cell death by oxidative stress in retinal pigment epithelial cells. *Cell Death & Disease*, *4*(12), e965–e965. https://doi.org/10.1038/cddis.2013.478

Harkin, K., Augustine, J., Stitt, A. W., Xu, H., & Chen, M. (2022). Wedelolactone Attenuates N-methyl-N-nitrosourea-Induced Retinal Neurodegeneration through Suppression of the AIM2/CASP11 Pathway. *Biomedicines*, *10*(2), 311.

https://doi.org/10.3390/biomedicines10020311

Harrison, S. A., Goodman, Z., Jabbar, A., Vemulapalli, R., Younes, Z. H., Freilich, B., Sheikh, M. Y., Schattenberg, J. M., Kayali, Z., Zivony, A., Sheikh, A., Garcia-Samaniego, J., Satapathy, S. K., Therapondos, G., Mena, E., Schuppan, D., Robinson, J., Chan, J. L., Hagerty, D. T., & Sanyal, A. J. (2020). A randomized, placebo-controlled trial of emricasan in patients with NASH and F1-F3 fibrosis. *Journal of Hepatology*, *72*(5), 816–827. https://doi.org/10.1016/j.jhep.2019.11.024

Higgins, G. T., Wang, J. H., Dockery, P., Cleary, P. E., & Redmond, H. P. (2003). Induction of Angiogenic Cytokine Expression in Cultured RPE by Ingestion of Oxidized Photoreceptor Outer Segments. *Investigative Opthalmology & Visual Science*, *44*(4), 1775. https://doi.org/10.1167/iovs.02-0742

Hinton, D., & Kannan, R. (2014). Sodium iodate induced retinal degeneration: new insights from an old model. *Neural Regeneration Research*, *9*(23), 2044. https://doi.org/10.4103/1673-5374.147927

Hisahara, S., Yuan, J., Momoi, T., Okano, H., & Miura, M. (2001). Caspase-11 Mediates Oligodendrocyte Cell Death and Pathogenesis of Autoimmune-Mediated Demyelination. *Journal of Experimental Medicine*, *193*(1), 111–122. https://doi.org/10.1084/jem.193.1.111

Höhn, A., & Grune, T. (2013). Lipofuscin: formation, effects and role of macroautophagy. *Redox Biology*, *1*(1), 140–144. https://doi.org/10.1016/j.redox.2013.01.006

Hoon, M., Okawa, H., Della Santina, L., & Wong, R. O. L. (2014). Functional architecture of the retina: Development and disease. *Progress in Retinal and Eye Research*, *42*, 44–84. https://doi.org/10.1016/j.preteyeres.2014.06.003

Hornung, V., Ablasser, A., Charrel-Dennis, M., Bauernfeind, F., Horvath, G., Caffrey, D. R., Latz, E., & Fitzgerald, K. A. (2009). AIM2 recognizes cytosolic dsDNA and forms a caspase-1-activating inflammasome with ASC. *Nature*, *458*(7237), 514–518. https://doi.org/10.1038/nature07725

Hytti, M., Korhonen, E., Hongisto, H., Kaarniranta, K., Skottman, H., & Kauppinen, A. (2021). Differential Expression of Inflammasome-Related Genes in Induced Pluripotent Stem-Cell-Derived Retinal Pigment Epithelial Cells with or without History of Age-Related Macular Degeneration. *International Journal of Molecular Sciences*, *22*(13), 6800. https://doi.org/10.3390/ijms22136800

Imamura, Y., Noda, S., Hashizume, K., Shinoda, K., Yamaguchi, M., Uchiyama, S., Shimizu, T., Mizushima, Y., Shirasawa, T., & Tsubota, K. (2006). Drusen, choroidal neovascularization, and retinal pigment epithelium dysfunction in SOD1-deficient mice: A model of age-related macular degeneration. *Proceedings of the National Academy of Sciences*, *103*(30), 11282–11287. https://doi.org/10.1073/pnas.0602131103

Jiang, M., Sun, X., Liu, S., Tang, Y., Shi, Y., Bai, Y., Wang, Y., Yang, Q., Yang, Q., Jiang, W., Yuan, H., Jiang, Q., & Cai, J. (2021). Caspase-11-Gasdermin D-Mediated Pyroptosis Is Involved in the Pathogenesis of Atherosclerosis. *Frontiers in Pharmacology*, *12*. https://doi.org/10.3389/fphar.2021.657486

Jorgensen, I., & Miao, E. A. (2015). Pyroptotic cell death defends against intracellular pathogens. *Immunological Reviews*, *265*(1), 130–142. https://doi.org/10.1111/imr.12287

Justilien, V., Pang, J.-J., Renganathan, K., Zhan, X., Crabb, J. W., Kim, S. R., Sparrow, J. R.,

Hauswirth, W. W., & Lewin, A. S. (2007). SOD2 Knockdown Mouse Model of Early AMD. *Investigative Opthalmology & Visual Science*, *48*(10), 4407. https://doi.org/10.1167/iovs.07-0432

Kadkhodaeian, H. A., Tiraihi, T., Daftarian, N., Ahmadieh, H., Ziaei, H., & Taheri, T. (2016). Histological and electrophysiological changes in the retinal pigment epithelium after injection of sodium iodate in the orbital venus plexus of pigmented rats. *Journal of Ophthalmic and Vision Research*, *11*(1), 70–77. https://doi.org/10.4103/2008-322X.180695

Kaneko, H., Dridi, S., Tarallo, V., Gelfand, B. D., Fowler, B. J., Cho, W. G., Kleinman, M. E., Ponicsan, S. L., Hauswirth, W. W., Chiodo, V. A., Karikó, K., Yoo, J. W., Lee, D., Hadziahmetovic, M., Song, Y., Misra, S., Chaudhuri, G., Buaas, F. W., Braun, R. E., … Ambati, J. (2011). DICER1 deficit induces Alu RNA toxicity in age-related macular degeneration. *Nature*, *471*(7338), 325–330. https://doi.org/10.1038/nature09830

Kauppinen, A., Niskanen, H., Suuronen, T., Kinnunen, K., Salminen, A., & Kaarniranta, K. (2012). Oxidative stress activates NLRP3 inflammasomes in ARPE-19 cells—Implications for age-related macular degeneration (AMD). *Immunology Letters*, *147*(1–2), 29–33. https://doi.org/10.1016/j.imlet.2012.05.005

Kayagaki, N., Stowe, I. B., Lee, B. L., O'Rourke, K., Anderson, K., Warming, S., Cuellar, T., Haley, B., Roose-Girma, M., Phung, Q. T., Liu, P. S., Lill, J. R., Li, H., Wu, J., Kummerfeld, S., Zhang, J., Lee, W. P., Snipas, S. J., Salvesen, G. S., … Dixit, V. M. (2015). Caspase-11 cleaves gasdermin D for non-canonical inflammasome signalling. *Nature*, *526*(7575), 666–671. https://doi.org/10.1038/nature15541

Kayagaki, N., Warming, S., Lamkanfi, M., Walle, L. Vande, Louie, S., Dong, J., Newton, K.,

Qu, Y., Liu, J., Heldens, S., Zhang, J., Lee, W. P., Roose-Girma, M., & Dixit, V. M. (2011). Non-canonical inflammasome activation targets caspase-11. *Nature*, *479*(7371), 117–121. https://doi.org/10.1038/nature10558

Kelley, N., Jeltema, D., Duan, Y., & He, Y. (2019). The NLRP3 Inflammasome: An Overview of Mechanisms of Activation and Regulation. *International Journal of Molecular Sciences*, *20*(13), 3328. https://doi.org/10.3390/ijms20133328

Kerur, N., Fukuda, S., Banerjee, D., Kim, Y., Fu, D., Apicella, I., Varshney, A., Yasuma, R., Fowler, B. J., Baghdasaryan, E., Marion, K. M., Huang, X., Yasuma, T., Hirano, Y., Serbulea, V., Ambati, M., Ambati, V. L., Kajiwara, Y., Ambati, K., … Ambati, J. (2018). cGAS drives noncanonical-inflammasome activation in age-related macular degeneration. *Nature Medicine*, *24*(1), 50–61. https://doi.org/10.1038/nm.4450

Kerur, N., Veettil, M. V., Sharma-Walia, N., Bottero, V., Sadagopan, S., Otageri, P., & Chandran, B. (2011). IFI16 Acts as a Nuclear Pathogen Sensor to Induce the Inflammasome in Response to Kaposi Sarcoma-Associated Herpesvirus Infection. *Cell Host & Microbe*, *9*(5), 363–375. https://doi.org/10.1016/j.chom.2011.04.008

Khare, S., Dorfleutner, A., Bryan, N. B., Yun, C., Radian, A. D., de Almeida, L., Rojanasakul, Y., & Stehlik, C. (2012). An NLRP7-Containing Inflammasome Mediates Recognition of Microbial Lipopeptides in Human Macrophages. *Immunity*, *36*(3), 464–476. https://doi.org/10.1016/j.immuni.2012.02.001

Kim, H. J., Montenegro, D., Zhao, J., & Sparrow, J. R. (2021). Bisretinoids of the Retina: Photo-Oxidation, Iron-Catalyzed Oxidation, and Disease Consequences. *Antioxidants*, *10*(9), 1382. https://doi.org/10.3390/antiox10091382

Kiuchi, K., Yoshizawa, K., Shikata, N., Moriguchi, K., & Tsubura, A. (2002). Morphologic

characteristics of retinal degeneration induced by sodium iodate in mice. *Current Eye Research*, *25*(6), 373–379. https://doi.org/10.1076/ceyr.25.6.373.14227

Kobori, M., Yang, Z., Gong, D., Heissmeyer, V., Zhu, H., Jung, Y.-K., Gakidis, M. A. M., Rao, A., Sekine, T., Ikegami, F., Yuan, C., & Yuan, J. (2004). Wedelolactone suppresses LPS-induced caspase-11 expression by directly inhibiting the IKK Complex. *Cell Death & Differentiation*, *11*(1), 123–130. https://doi.org/10.1038/sj.cdd.4401325

Kocaoglu, O. P., Liu, Z., Zhang, F., Kurokawa, K., Jonnal, R. S., & Miller, D. T. (2016). Photoreceptor disc shedding in the living human eye. *Biomedical Optics Express*, *7*(11), 4554. https://doi.org/10.1364/BOE.7.004554

Koster, C., van den Hurk, K. T., ten Brink, J. B., Lewallen, C. F., Stanzel, B. V., Bharti, K., & Bergen, A. A. (2022). Sodium-Iodate Injection Can Replicate Retinal Degenerative Disease Stages in Pigmented Mice and Rats: Non-Invasive Follow-Up Using OCT and ERG. *International Journal of Molecular Sciences*, *23*(6), 2918. https://doi.org/10.3390/ijms23062918

Kostic, C., & Arsenijevic, Y. (2016). Animal modelling for inherited central vision loss. *The Journal of Pathology*, *238*(2), 300–310. https://doi.org/10.1002/path.4641

Krebs, I., Glittenberg, C., Ansari-Shahrezaei, S., Hagen, S., Steiner, I., & Binder, S. (2013). Non-responders to treatment with antagonists of vascular endothelial growth factor in age-related macular degeneration. *British Journal of Ophthalmology*, *97*(11), 1443–1446. https://doi.org/10.1136/bjophthalmol-2013-303513

Kudelova, J., Fleischmannova, J., Adamova, E., & Matalova, E. (2015). Pharmacological caspase inhibitors: research towards therapeutic perspectives. *J Physiol Pharmacol*, *66*(4), 473–482.

Lad, E. M., Cousins, S. W., Van Arnam, J. S., & Proia, A. D. (2015). Abundance of infiltrating CD163+ cells in the retina of postmortem eyes with dry and neovascular age-related macular degeneration. *Graefe's Archive for Clinical and Experimental Ophthalmology*, *253*(11), 1941–1945. https://doi.org/10.1007/s00417-015-3094-z

Lawlor, K. E., Khan, N., Mildenhall, A., Gerlic, M., Croker, B. A., D'Cruz, A. A., Hall, C., Kaur Spall, S., Anderton, H., Masters, S. L., Rashidi, M., Wicks, I. P., Alexander, W. S., Mitsuuchi, Y., Benetatos, C. A., Condon, S. M., Wong, W. W.-L., Silke, J., Vaux, D. L., & Vince, J. E. (2015). RIPK3 promotes cell death and NLRP3 inflammasome activation in the absence of MLKL. *Nature Communications*, *6*(1), 6282. https://doi.org/10.1038/ncomms7282

Lee, J. E., Liang, K. J., Fariss, R. N., & Wong, W. T. (2008). Ex Vivo Dynamic Imaging of Retinal Microglia Using Time-Lapse Confocal Microscopy. *Investigative Ophthalmology & Visual Science*, *49*(9), 4169–4176. https://doi.org/10.1167/iovs.08-2076

Li, J., McQuade, T., Siemer, A. B., Napetschnig, J., Moriwaki, K., Hsiao, Y.-S., Damko, E., Moquin, D., Walz, T., McDermott, A., Chan, F. K.-M., & Wu, H. (2012). The RIP1/RIP3 Necrosome Forms a Functional Amyloid Signaling Complex Required for Programmed Necrosis. *Cell*, *150*(2), 339–350. https://doi.org/10.1016/j.cell.2012.06.019

Li, L., Xing, C., Zhou, J., Niu, L., Luo, B., Song, M., Niu, J., Ruan, Y., Sun, X., & Lei, Y. (2021). Airborne particulate matter (PM2.5) triggers ocular hypertension and glaucoma through pyroptosis. *Particle and Fibre Toxicology*, *18*(1), 10. https://doi.org/10.1186/s12989-021-00403-4

Li, Y., Fu, T.-M., Lu, A., Witt, K., Ruan, J., Shen, C., & Wu, H. (2018). Cryo-EM structures of ASC and NLRC4 CARD filaments reveal a unified mechanism of nucleation and activation of caspase-1. *Proceedings of the National Academy of Sciences*, *115*(43), 10845–10852. https://doi.org/10.1073/pnas.1810524115

Li, Y., Huang, T.-T., Carlson, E. J., Melov, S., Ursell, P. C., Olson, J. L., Noble, L. J., Yoshimura, M. P., Berger, C., Chan, P. H., Wallace, D. C., & Epstein, C. J. (1995). Dilated cardiomyopathy and neonatal lethality in mutant mice lacking manganese superoxide dismutase. *Nature Genetics*, *11*(4), 376–381. https://doi.org/10.1038/ng1295-376

Lim, R. R., Wieser, M. E., Ganga, R. R., Barathi, V. A., Lakshminarayanan, R., Mohan, R. R., Hainsworth, D. P., & Chaurasia, S. S. (2020). NOD-like Receptors in the Eye: Uncovering Its Role in Diabetic Retinopathy. *International Journal of Molecular Sciences*, *21*(3), 899. https://doi.org/10.3390/ijms21030899

Lu, Y., Hu, D., Ma, S., Zhao, X., Wang, S., Wei, G., Wang, X., Wen, A., & Wang, J. (2016). Protective effect of wedelolactone against CCl 4 -induced acute liver injury in mice. *International Immunopharmacology*, *34*, 44–52. https://doi.org/10.1016/j.intimp.2016.02.003

Machalińska, A., Lubiński, W., Kłos, P., Kawa, M., Baumert, B., Penkala, K., Grzegrzółka, R., Karczewicz, D., Wiszniewska, B., & Machaliński, B. (2010). Sodium Iodate Selectively Injuries the Posterior Pole of the Retina in a Dose-Dependent Manner: Morphological and Electrophysiological Study. *Neurochemical Research*, *35*(11), 1819–1827. https://doi.org/10.1007/s11064-010-0248-6

MacKenzie, S. H., Schipper, J. L., & Clark, A. C. (2010). The potential for caspases in drug

discovery. *Current Opinion in Drug Discovery & Development*, *13*(5), 568–576. http://www.ncbi.nlm.nih.gov/pubmed/20812148

Mao, H., Seo, S. J., Biswal, M. R., Li, H., Conners, M., Nandyala, A., Jones, K., Le, Y.-Z., & Lewin, A. S. (2014). Mitochondrial Oxidative Stress in the Retinal Pigment Epithelium Leads to Localized Retinal Degeneration. *Investigative Opthalmology & Visual Science*, *55*(7), 4613. https://doi.org/10.1167/iovs.14-14633

Mao, X., Pan, T., Shen, H., Xi, H., Yuan, S., & Liu, Q. (2018). The rescue effect of mesenchymal stem cell on sodium iodate-induced retinal pigment epithelial cell death through deactivation of NF-κB-mediated NLRP3 inflammasome. *Biomedicine & Pharmacotherapy*, *103*, 517–523. https://doi.org/10.1016/j.biopha.2018.04.038

Martinon, F., Burns, K., & Tschopp, J. (2002). The inflammasome: a molecular platform triggering activation of inflammatory caspases and processed of proIL-beta. *Molecular Cell*, *10*(2), 417–426.

Martinon, F., Mayor, A., & Tschopp, J. (2009). The Inflammasomes: Guardians of the Body. *Annual Review of Immunology*, *27*(1), 229–265. https://doi.org/10.1146/annurev.immunol.021908.132715

Matsuoka, Y., Yamashita, A., Matsuda, M., Kawai, K., Sawa, T., & Amaya, F. (2019). NLRP2 inflammasome in dorsal root ganglion as a novel molecular platform that produces inflammatory pain hypersensitivity. *Pain*, *160*(9), 2149–2160. https://doi.org/10.1097/j.pain.0000000000001611

Medzhitov, R. (2008). Origin and physiological roles of inflammation. *Nature*, *454*(7203), 428–435. https://doi.org/10.1038/nature07201

Merker, K., & Grune, T. (2000). Proteolysis of oxidised proteins and cellular senescence. *Experimental Gerontology*, *35*(6–7), 779–786. https://doi.org/10.1016/S0531-5565(00)00140-6

Miao, H., Tao, Y., & Li, X. X. (2012). Inflammatory cytokines in aqueous humor of patients with choroidal neovascularization. *Molecular Vision*, *18*(October 2011), 574–580.

Miao, N., Yin, F., Xie, H., Wang, Y., Xu, Y., Shen, Y., Xu, D., Yin, J., Wang, B., Zhou, Z., Cheng, Q., Chen, P., Xue, H., Zhou, L., Liu, J., Wang, X., Zhang, W., & Lu, L. (2019). The cleavage of gasdermin D by caspase-11 promotes tubular epithelial cell pyroptosis and urinary IL-18 excretion in acute kidney injury. *Kidney International*, *96*(5), 1105–1120. https://doi.org/10.1016/j.kint.2019.04.035

Mitchell, P., Liew, G., Gopinath, B., & Wong, T. Y. (2018). Age-related macular degeneration. *The Lancet*, *392*(10153), 1147–1159. https://doi.org/10.1016/S0140-6736(18)31550-2

Mohr, S., Xi, X., Tang, J., & Kern, T. S. (2002). Caspase Activation in Retinas of Diabetic and Galactosemic Mice and Diabetic Patients. *Diabetes*, *51*(4), 1172–1179. https://doi.org/10.2337/diabetes.51.4.1172

Monés, J., Leiva, M., Peña, T., Martínez, G., Biarnés, M., Garcia, M., Serrano, A., & Fernandez, E. (2016). A Swine Model of Selective Geographic Atrophy of Outer Retinal Layers Mimicking Atrophic AMD: A Phase I Escalating Dose of Subretinal Sodium Iodate. *Investigative Opthalmology & Visual Science*, *57*(10), 3974. https://doi.org/10.1167/iovs.16-19355

Mulfaul, K., Rhatigan, M., & Doyle, S. (2018). *Toll-Like Receptors and Age-Related Macular Degeneration* (pp. 19–28). https://doi.org/10.1007/978-3-319-75402-4_3

Natoli, R., Jiao, H., Barnett, N. L., Fernando, N., Valter, K., Provis, J. M., & Rutar, M. (2016). A model of progressive photo-oxidative degeneration and inflammation in the pigmented C57BL/6J mouse retina. *Experimental Eye Research*, *147*, 114–127. https://doi.org/10.1016/j.exer.2016.04.015

Noel, J. M., Fernandez de Castro, J. P., DeMarco, P. J., Franco, L. M., Wang, W., Vukmanic, E. V., Peng, X., Sandell, J. H., Scott, P. A., Kaplan, H. J., & McCall, M. A. (2012). Iodoacetic acid, but not sodium iodate, creates an inducible swine model of photoreceptor damage. *Experimental Eye Research*, *97*(1), 137–147. https://doi.org/10.1016/j.exer.2011.12.018

Noell, W. (1953). Experimentally induced toxic effects on structure and function of visual cells and pigment epithelium. *American Journal of Ophthalmology*, *36*(6), 103–116.

Organisciak, D. T., & Winkler, B. S. (1994). Retinal light damage: Practical and theoretical considerations. *Progress in Retinal and Eye Research*, *13*(1), 1–29. https://doi.org/10.1016/1350-9462(94)90003-5

Osterloh, J. M., Yang, J., Rooney, T. M., Fox, A. N., Adalbert, R., Powell, E. H., Sheehan, A. E., Avery, M. A., Hackett, R., Logan, M. A., MacDonald, J. M., Ziegenfuss, J. S., Milde, S., Hou, Y.-J., Nathan, C., Ding, A., Brown, R. H., Conforti, L., Coleman, M., … Freeman, M. R. (2012). dSarm/Sarm1 Is Required for Activation of an Injury-Induced Axon Death Pathway. *Science*, *337*(6093), 481–484. https://doi.org/10.1126/science.1223899

Ozaki, E., Gibbons, L., Neto, N. G., Kenna, P., Carty, M., Humphries, M., Humphries, P., Campbell, M., Monaghan, M., Bowie, A., & Doyle, S. L. (2020). SARM1 deficiency promotes rod and cone photoreceptor cell survival in a model of retinal

degeneration. *Life Science Alliance*, *3*(5), e201900618. https://doi.org/10.26508/lsa.201900618

Pan, H., Lin, Y., Dou, J., Fu, Z., Yao, Y., Ye, S., Zhang, S., Wang, N., Liu, A., Li, X., Zhang, F., & Chen, D. (2020). Wedelolactone facilitates Ser/Thr phosphorylation of NLRP3 dependent on PKA signalling to block inflammasome activation and pyroptosis. *Cell Proliferation*, *53*(9). https://doi.org/10.1111/cpr.12868

Pascolini, D., & Mariotti, S. P. (2012). Global estimates of visual impairment: 2010. *British Journal of Ophthalmology*, *96*(5), 614–618. https://doi.org/10.1136/bjophthalmol-2011-300539

Raoul, W., Auvynet, C., Camelo, S., Guillonneau, X., Feumi, C., Combadière, C., & Sennlaub, F. (2010). CCL2/CCR2 and CX3CL1/CX3CR1 chemokine axes and their possible involvement in age-related macular degeneration. *Journal of Neuroinflammation*, *7*(1), 87. https://doi.org/10.1186/1742-2094-7-87

Rastoin, O., Pagès, G., & Dufies, M. (2020). Experimental Models in Neovascular Age Related Macular Degeneration. *International Journal of Molecular Sciences*, *21*(13), 4627. https://doi.org/10.3390/ijms21134627

Rozanowski, B., Burke, J. M., Boulton, M. E., Sarna, T., & Rozanowska, M. (2008). Human RPE Melanosomes Protect from Photosensitized and Iron-Mediated Oxidation but Become Pro-oxidant in the Presence of Iron upon Photodegradation. *Investigative Ophthalmology & Visual Science*, *49*(7), 2838–2847. https://doi.org/10.1167/iovs.08-1700

Rühl, S., & Broz, P. (2015). Caspase-11 activates a canonical NLRP3 inflammasome by promoting K + efflux. *European Journal of Immunology*, *45*(10), 2927–2936.

https://doi.org/10.1002/eji.201545772

Sabour-Pickett, S., Beatty, S., Connolly, E., Loughman, J., Stack, J., Howard, A., Klein, R., Klein, B. E., Meuer, S. M., Myers, C. E., Akuffo, K. O., & Nolan, J. M. (2014). SUPPLEMENTATION WITH THREE DIFFERENT MACULAR CAROTENOID FORMULATIONS IN PATIENTS WITH EARLY AGE-RELATED MACULAR DEGENERATION. *Retina*, *34*(9), 1757–1766. https://doi.org/10.1097/IAE.0000000000000174

Sagulenko, V., Thygesen, S. J., Sester, D. P., Idris, A., Cridland, J. A., Vajjhala, P. R., Roberts, T. L., Schroder, K., Vince, J. E., Hill, J. M., Silke, J., & Stacey, K. J. (2013). AIM2 and NLRP3 inflammasomes activate both apoptotic and pyroptotic death pathways via ASC. *Cell Death & Differentiation*, *20*(9), 1149–1160. https://doi.org/10.1038/cdd.2013.37

Schnabolk, G., Obert, E., Banda, N. K., & Rohrer, B. (2020). Systemic Inflammation by Collagen-Induced Arthritis Affects the Progression of Age-Related Macular Degeneration Differently in Two Mouse Models of the Disease. *Investigative Opthalmology & Visual Science*, *61*(14), 11. https://doi.org/10.1167/iovs.61.14.11

Schütt, F., Bergmann, M., Holz, F. G., & Kopitz, J. (2002). Isolation of intact lysosomes from human RPE cells and effects of A2-E on the integrity of the lysosomal and other cellular membranes. *Graefe's Archive for Clinical and Experimental Ophthalmology*, *240*(12), 983–988. https://doi.org/10.1007/s00417-002-0558-8

Shi, J., Zhao, Y., Wang, K., Shi, X., Wang, Y., Huang, H., Zhuang, Y., Cai, T., Wang, F., & Shao, F. (2015). Cleavage of GSDMD by inflammatory caspases determines pyroptotic cell death. *Nature*, *526*(7575), 660–665.

https://doi.org/10.1038/nature15514

Shi, J., Zhao, Y., Wang, Y., Gao, W., Ding, J., Li, P., Hu, L., & Shao, F. (2014). Inflammatory caspases are innate immune receptors for intracellular LPS. *Nature*, *514*(7521), 187–192. https://doi.org/10.1038/nature13683

Sies, H., Berndt, C., & Jones, D. P. (2017). Oxidative Stress. *Annual Review of Biochemistry*, *86*(1), 715–748. https://doi.org/10.1146/annurev-biochem-061516-045037

Silke, E., Cahill, M., Campbell, M., & Doyle, S. L. (2023). Inflammasomes in the pathobiology of degenerative retinopathies. In *Inflammasome Biology* (pp. 465–485). Elsevier. https://doi.org/10.1016/B978-0-323-91802-2.00021-9

Smith, A. P., & Creagh, E. M. (2022). Caspase-4 and -5 Biology in the Pathogenesis of Inflammatory Bowel Disease. *Frontiers in Pharmacology*, *13*. https://doi.org/10.3389/fphar.2022.919567

Sorsby, A. (1941). Experimental Pigmentary Degeneration of the Retina by Sodium Iodate. *The British Journal of Ophthalmology*, *25*(2), 58–62.

Strauss, O. (2005). The Retinal Pigment Epithelium in Visual Function. *Physiological Reviews*, *85*(3), 845–881. https://doi.org/10.1152/physrev.00021.2004

Suzuki, M., Kamei, M., Itabe, H., Yoneda, K., Bando, H., Kume, N., & Tano, Y. (2007). Oxidized phospholipids in the macula increase with age and in eyes with age-related macular degeneration. *Molecular Vision*, *13*, 772–778. http://www.ncbi.nlm.nih.gov/pubmed/17563727

Tarallo, V., Hirano, Y., Gelfand, B. D., Dridi, S., Kerur, N., Kim, Y., Cho, W. G., Kaneko, H.,

Fowler, B. J., Bogdanovich, S., Albuquerque, R. J. C., Hauswirth, W. W., Chiodo, V. A., Kugel, J. F., Goodrich, J. A., Ponicsan, S. L., Chaudhuri, G., Murphy, M. P., Dunaief, J. L., … Ambati, J. (2012). DICER1 Loss and Alu RNA Induce Age-Related Macular Degeneration via the NLRP3 Inflammasome and MyD88. *Cell*, *149*(4), 847–859. https://doi.org/10.1016/j.cell.2012.03.036

Thomas, D. C. (2017). The phagocyte respiratory burst: Historical perspectives and recent advances. *Immunology Letters*, *192*, 88–96. https://doi.org/10.1016/j.imlet.2017.08.016

Thornton, J., Edwards, R., Mitchell, P., Harrison, R. A., Buchan, I., & Kelly, S. P. (2005). Smoking and age-related macular degeneration: a review of association. *Eye*, *19*(9), 935–944. https://doi.org/10.1038/sj.eye.6701978

Tseng, W. A., Thein, T., Kinnunen, K., Lashkari, K., Gregory, M. S., D'Amore, P. A., & Ksander, B. R. (2013). NLRP3 Inflammasome Activation in Retinal Pigment Epithelial Cells by Lysosomal Destabilization: Implications for Age-Related Macular Degeneration. *Investigative Opthalmology & Visual Science*, *54*(1), 110. https://doi.org/10.1167/iovs.12-10655

Tsuruma, K., Yamauchi, M., Inokuchi, Y., Sugitani, S., Shimazawa, M., & Hara, H. (2012). Role of Oxidative Stress in Retinal Photoreceptor Cell Death in N-Methyl-N-nitrosourea–Treated Mice. *Journal of Pharmacological Sciences*, *118*(3), 351–362. https://doi.org/10.1254/jphs.11110FP

Tuo, J., Bojanowski, C. M., Zhou, M., Shen, D., Ross, R. J., Rosenberg, K. I., Cameron, D. J., Yin, C., Kowalak, J. A., Zhuang, Z., Zhang, K., & Chan, C.-C. (2007). Murine Ccl2/Cx3cr1 Deficiency Results in Retinal Lesions Mimicking Human Age-Related

Macular Degeneration. *Investigative Opthalmology & Visual Science*, *48*(8), 3827. https://doi.org/10.1167/iovs.07-0051

Tuo, J., Smith, B. C., Bojanowski, C. M., Meleth, A. D., Gery, I., Csaky, K. G., Chew, E. Y., & Chan, C.-C. (2004). The involvement of sequence variation and expression of CX3CR1 in the pathogenesis of age-related macular degeneration. *The FASEB Journal*, *18*(11), 1297–1299. https://doi.org/10.1096/fj.04-1862fje

Ufret-Vincenty, R. L., Aredo, B., Liu, X., McMahon, A., Chen, P. W., Sun, H., Niederkorn, J. Y., & Kedzierski, W. (2010). Transgenic Mice Expressing Variants of Complement Factor H Develop AMD-like Retinal Findings. *Investigative Opthalmology & Visual Science*, *51*(11), 5878. https://doi.org/10.1167/iovs.09-4457

Van Noorden, C. J. F. (2001). The history of Z-VAD-FMK, a tool for understanding the significance of caspase inhibition. *Acta Histochemica*, *103*(3), 241–251. https://doi.org/10.1078/0065-1281-00601

Vance, R. E. (2015). The NAIP/NLRC4 inflammasomes. *Current Opinion in Immunology*, *32*, 84–89. https://doi.org/10.1016/j.coi.2015.01.010

Vladimer, G. I., Weng, D., Paquette, S. W. M., Vanaja, S. K., Rathinam, V. A. K., Aune, M. H., Conlon, J. E., Burbage, J. J., Proulx, M. K., Liu, Q., Reed, G., Mecsas, J. C., Iwakura, Y., Bertin, J., Goguen, J. D., Fitzgerald, K. A., & Lien, E. (2012). The NLRP12 Inflammasome Recognizes Yersinia pestis. *Immunity*, *37*(1), 96–107. https://doi.org/10.1016/j.immuni.2012.07.006

Volland, S., Esteve-Rudd, J., Hoo, J., Yee, C., & Williams, D. S. (2015). A Comparison of Some Organizational Characteristics of the Mouse Central Retina and the Human Macula. *PLOS ONE*, *10*(4), e0125631.

https://doi.org/10.1371/journal.pone.0125631

Wang, J., Iacovelli, J., Spencer, C., & Saint-Geniez, M. (2014). Direct Effect of Sodium Iodate on Neurosensory Retina. *Investigative Opthalmology & Visual Science*, *55*(3), 1941. https://doi.org/10.1167/iovs.13-13075

Wang, W., Noel, J., Kaplan, H. J., & Dean, D. C. (2011). Circulating Reactive Oxidant Causes Apoptosis of Retinal Pigment Epithelium and Cone Photoreceptors in the Mouse Central Retina. *Ophthalmology and Eye Diseases*, *3*, OED.S7797. https://doi.org/10.4137/OED.S7797

Weaver, C., Cyr, B., de Rivero Vaccari, J. C., & de Rivero Vaccari, J. P. (2020). Inflammasome Proteins as Inflammatory Biomarkers of Age-Related Macular Degeneration. *Translational Vision Science & Technology*, *9*(13), 27. https://doi.org/10.1167/tvst.9.13.27

Wooff, Y., Fernando, N., Wong, J. H. C., Dietrich, C., Aggio-Bruce, R., Chu-Tan, J. A., Robertson, A. A. B., Doyle, S. L., Man, S. M., & Natoli, R. (2020). Caspase-1-dependent inflammasomes mediate photoreceptor cell death in photo-oxidative damage-induced retinal degeneration. *Scientific Reports*, *10*(1), 1–20. https://doi.org/10.1038/s41598-020-58849-z

Xu, H., Chen, M., & Forrester, J. V. (2009). Para-inflammation in the aging retina. *Progress in Retinal and Eye Research*, *28*(5), 348–368. https://doi.org/10.1016/j.preteyeres.2009.06.001

Xu, S., Liu, X., Liu, X., Shi, Y., Jin, X., Zhang, N., Li, X., & Zhang, H. (2021). Wedelolactone ameliorates Pseudomonas aeruginosa-induced inflammation and corneal injury by suppressing caspase-4/5/11/GSDMD-mediated non-canonical pyroptosis.

*Experimental Eye Research*, *211*, 108750. https://doi.org/10.1016/j.exer.2021.108750

Yang, X., Rai, U., Chung, J.-Y., & Esumi, N. (2021). Fine Tuning of an Oxidative Stress Model with Sodium Iodate Revealed Protective Effect of NF-κB Inhibition and Sex-Specific Difference in Susceptibility of the Retinal Pigment Epithelium. *Antioxidants*, *11*(1), 103. https://doi.org/10.3390/antiox11010103

Yi, Y. S. (2020). Caspase-11 non-canonical inflammasome: Emerging activator and regulator of infection-mediated inflammatory responses. *International Journal of Molecular Sciences*, *21*(8), 1–11. https://doi.org/10.3390/ijms21082736

Young, B. M., Jones, K., Massengill, M. T., Walsh, E., Li, H., Lewin, A. S., & Ildefonso, C. J. (2019). Expression of a CARD Slows the Retinal Degeneration of a Geographic Atrophy Mouse Model. *Molecular Therapy - Methods & Clinical Development*, *14*, 113–125. https://doi.org/10.1016/j.omtm.2019.06.001

Zanoni, I., Tan, Y., Di Gioia, M., Broggi, A., Ruan, J., Shi, J., Donado, C. A., Shao, F., Wu, H., Springstead, J. R., & Kagan, J. C. (2016). An endogenous caspase-11 ligand elicits interleukin-1 release from living dendritic cells. *Science*, *352*(6290), 1232–1236. https://doi.org/10.1126/science.aaf3036

Zhang, N., Zhang, X., Girardot, P. E., Chrenek, M. A., Sellers, J. T., Li, Y., Kim, Y.-K., Summers, V. R., Ferdous, S., Shelton, D. A., Boatright, J. H., & Nickerson, J. M. (2021). Electrophysiologic and Morphologic Strain Differences in a Low-Dose NaIO 3 -Induced Retinal Pigment Epithelium Damage Model. *Translational Vision Science & Technology*, *10*(8), 10. https://doi.org/10.1167/tvst.10.8.10

Zheng, D., Kern, L., & Elinav, E. (2021). The NLRP6 inflammasome. *Immunology*, *162*(3),

281–289. https://doi.org/10.1111/imm.13293

Zhou, H., Zhang, H., Yu, A., & Xie, J. (2018). Association between sunlight exposure and risk of age-related macular degeneration: a meta-analysis. *BMC Ophthalmology*, *18*(1), 331. https://doi.org/10.1186/s12886-018-1004-y